TECHNICAL PAPER

fib WILEY

Predictive model for slenderness limit of circular RC columns confined with FRP wraps

Alireza Arabshahi | **Mohammadreza Tavakkolizadeh** [ID]

Civil Engineering Department, Ferdowsi University of Mashhad, Mashhad, Iran

Correspondence
Mohammadreza Tavakkolizadeh, Civil Engineering Department, Ferdowsi University of Mashhad, Mashhad, Iran.
Email: drt@um.ac.ir

Funding information
Faculty of Engineering at Ferdowsi University of Mashhad, Grant/Award Number: 52205

Abstract

Application of fiber-reinforced polymer (FRP) for retrofitting and rehabilitation of concrete structures is a common method. The main role of FRP confinement for reinforced concrete (RC) columns is to increase the ultimate strength and strain of confined concrete core and therefore improve in the load carrying capacity of the columns. However, it is possible that a previously short column fails due to buckling after the application of FRP confinement. In other words, the enhanced compressive strength of a retrofitted column may go beyond its buckling load. Therefore, a design criterion to predict this condition is necessary for the designers in the preliminary and final stages of the design. In this paper, a predictive model is proposed to determine the slenderness limit of FRP-confined circular RC columns. The suggested relation was derived using one of the accurate design-oriented strength models for FRP-confined concrete columns as well as analytically derived buckling equations. The effect of hybrid FRP confinement is also incorporated in the suggested slenderness limit. Moreover, a parametric study was performed on the suggested model to specify most influential parameters. The accuracy of the proposed relation was evaluated using a database of experimental results collected from previous studies. The results of the evaluations demonstrated acceptable accuracy of the proposed relation in predicting behavior and failure mode of FRP-confined RC columns.

KEYWORDS
buckling, circular RC column, FRP confined strength, hybrid confinement, slenderness limit

1 | INTRODUCTION

Due to the desirable characteristics of fiber-reinforced polymer (FRP) materials such as high-tensile strength, corrosion resistance, lightweight, and ease of application, using them for strengthening and rehabilitation of existing reinforced concrete (RC) structural elements becomes an attractive method. Accordingly, in the past three decades, various studies have been performed on different aspects of FRP applications in concrete structures.[1–3] Many of the existing studies deal with the FRP strengthening of concrete columns.[4–10] The concrete members, especially columns, usually require strengthening because of loading eccentricity, impact or seismic loads, or being exposed to harsh environments such as saltwater, chemical substances, or temperature cycles. Accordingly, various studies have been performed on application of FRP sheets and tubes for

improving the performance of concrete structural components.[11–17] For instance, in one of the recent studies on FRP-confined columns, Wang et al.[11] experimentally investigated the performance of CFRP-wrapped RC columns with rectangular sections under eccentrical loads, considering the effects of preloading level. Mai et al.[12] studied the nonuniform wrapping techniques for improving the failure strength of FRP-confined rectangular columns. The effect of partial CFRP confinement on the performance of concrete columns made of seawater and sea-sand aggregates is investigated by Yang et al.[13] Mai et al.[14] studied the behavior of partially confined square columns under different loading conditions. Pham et al.[15] evaluated the effects of different wrapping methods on compressive strength of FRP-confined circular concrete columns.

Many of the performed studies on FRP-confined concrete have been concentrated on development of predictive models for the stress and strain behavior of confined concrete. [18–20] One of the factors that affect the performance of confined concrete is the path dependence behavior of concrete.[21] However, in most of the available models for confined concrete, it is assumed that the confined axial stress of concrete is independent on the loading path history, and accordingly the progressive development of tensile splitting cracks in confined concrete is ignored.[22,23] Recent studies proved that due to the progressive formation of tensile splitting crack by increase in the axial strain, which in turn depends on different factors mainly the wet packing density,[24,25] the degree of splitting crack at a given confining stress in passively confined concrete should be larger and hence, passively confined concrete experience a smaller axial stress than that in the actively confined concrete.[1] In this regard, attempts have been made recently to include the effect of the path dependence on the stress–strain models and behavior of FRP-confined concrete.[26,27]

It is known that FRP wraps increase the strength and ductility of concrete columns, but this effect in wrapped slender columns is not as significant as in the short ones. Therefore, it seems rational to find slenderness limits for concrete columns, which beyond them, the FRP wrapping is not very efficient for improving strength and ductility. Retrofitting slender FRP-confined RC columns is a common challenge for the designers because all design specifications and codes only consider short columns and are silenced in regard to the effects of slenderness.[28–30]

1.1 | Review of the previous studies on slender confined columns

In the past decade, few researchers have investigated the performance of slender FRP-confined RC columns, experimentally, analytically, and numerically. For instance, Pan et al.[31] conducted axial compression tests on slender rectangular FRP-confined RC columns with slenderness ratio varying from 4.5 to 17.5. They concluded that in comparison with ordinary RC columns, the FRP-confined columns are more susceptible to the negative effects of slenderness. They also used the ANSYS software package to numerically investigate the performance of slender FRP-confined columns and performed a parametric study considering the effect of parameters such as cross-section area, confinement ratio, and reinforcing ratio. Based on their attained results, they proposed a simplified formula to calculate the stability coefficient for FRP-confined rectangular columns. To remove the restrictions of the existing provisions for the design of FRP-confined RC columns to only short columns, Jiang and Teng[32] suggested a theoretical model for slender circular concrete columns. Numerical validations demonstrated that their proposed model is in good agreement with existing experimental test results on slender columns. In another research, Siddiqui et al.[33] performed an extended experimental study on slender FRP confined RC columns to determine the effects of the hoop and longitudinal FRP laminates on improving compressive strength and reducing lateral deflection of slender columns. They concluded that in the post-yielding phase, the longitudinal FRP laminates were more influential on load carrying capacity than the hoop FRP laminates. Based on their experiments, they tried to modify the ACI slenderness limit for RC columns to be applicable for analysis of columns confined with FRP laminates. Karimi et al.[34] suggested a novel composite steel-concrete-FRP column made of concrete-filled FRP tube with a steel section core. They performed a parametric study to investigate the effect of different parameters such as column diameter, FRP tube thickness, axial compressive modulus of the FRP tube, and ratio of steel-to-concrete area on the slenderness limit. Ali[35] studied the reliability of FRP-confined short and slender RC columns using the first-order reliability method. He utilized the finite difference method for structural analysis considering both material and geometrical nonlinearities. He used the load and resistance factors based on ACI assumptions and calculated reliability indexes for both confined and unconfined columns. He found that the application of FRP confinement improves the reliability of RC columns considerably. Hales et al.[36] proposed an analytical buckling model that was applicable for developing interaction diagrams for FRP spiral-confined circular concrete columns with various slenderness ratios, reinforced with steel, FRP, or both rebars. Al-Nimry and Soman[37] examined the slenderness effect on the performance of eccentrically loaded RC columns confined with FRP laminates. They tested the accuracy of

the stress–strain model used by ACI for estimating the axial strength of FRP confined slender RC columns and concluded that the mentioned model overestimates the ultimate capacity. Gajdošová and Bilčík[38] studied the effect of different types of CFRP wrapping on the performance of slender concrete columns.

1.2 | The objective of the present study

In addition to the abovementioned research works, many other studies are also conducted on the design and performance of FRP-confined slender reinforced or plain concrete columns.[39–43] Based on the findings of these studies, it is concluded that a short RC column can behave like a slender column after the addition of FRP wraps due to the increase in concrete compressive strength as result of the FRP confinement. In other words, if a short column supposed to fail by concrete crushing before the addition of FRP wraps, it might experience buckling, which usually occurs in slender columns, due to an increase in its load carrying capacity. Therefore, the need for a practical slenderness limit to help engineers to go through design procedure by using practical relations and easy to follow guide.

The main objective of the present study is to propose a new analytically derived relation to determine the slenderness limit for FRP confined circular RC columns. For this purpose, the buckling load of an RC column is set equal to its confined compressive load carrying capacity. One of the accurate design-oriented models for strength of confined concrete is used to calculate the compressive strength of FRP-confined RC column. Considering the concept of elasto-plastic buckling, lower and upperbound slenderness limits were derived for confined RC columns. The proposed relation has distinctive features in comparison with the other existing limits. First, the effect of different types of longitudinal reinforcement as well as the application of hybrid FRP confinement is incorporated in the development of the proposed relation. Moreover, using the results of the previous experimental studies, modifying coefficients were applied in the process of calculating various geometrical and material properties, which improved the accuracy of the proposed relation. A database of experimental results collected from the previous experimental studies on slender and short confined RC columns was used to verify accuracy of the proposed relations. Finally, a brief parametric study was performed on the suggested relation to determine the most influential parameters on the slenderness limit of confined circular RC columns in order to simplify the final relation.

2 | MODELING OF CONFINED PLAIN CONCRETE BEHAVIOR

The prerequisites for the development of slenderness limit for FRP-confined RC circular column are relations to predict ultimate strength, strain, as well as the bilinear stress–strain curve of FRP-confined concrete in compression. Several existing models and relations are available in literature; however, due to the sensitivity of the ultimate load carrying capacity to that strength, it is necessary to choose a model with the highest accuracy. In the present study, the following relations, which are proposed by Arabshahi et al.[8] and proved to have favorable performance, were used:

$$f_{cc} = f_{co} + \frac{39 f_l}{\ln^2(f_{co})}, \tag{1}$$

$$\varepsilon_{cu} = \frac{0.21 f_l^{0.68}}{f_{co} - \ln(\varepsilon_{co})}, \tag{2}$$

where, f_{cc} and f_{co} are the confined and unconfined concrete compressive strength, respectively. Similarly, ε_{cu} and ε_{co} are the ultimate strains of confined and unconfined concrete respectively. f_l is the confinement pressure, which is derived from the following relation:

$$f_l = \frac{2 f_f t_f}{d}, \tag{3}$$

where f_f and t_f are ultimate tensile strength and the total thickness of the FRP wraps, respectively, and d is the diameter of the concrete column.

Although the complete stress–strain curve of the confined concrete is not required directly in the process of deriving the slenderness limit, but as it will be discussed in the next sections, the first and second slopes of the stress–strain curve are used in derivation of the reduced modulus of elasticity for the confined concrete. Therefore, accuracy of the utilized model for predicting the stress–strain curve of the confined concrete will affect accuracy of the predicted slenderness limit. In the present study, the stress–strain curve of confined concrete, a modified version of well-known Richard and Abbot model[44] was used as follow:[8]

$$f_c = \frac{(E_1 - E_2)\varepsilon_c}{\left[1 + \left(\frac{(E_1 - E_2)\varepsilon_c}{f_0}\right)^{n_t}\right]^{\frac{1}{n_t}}} + E_2 \varepsilon_c. \tag{4}$$

$$E_1 = 3535 \sqrt{f_{co}} - f_{co}. \tag{5}$$

$$E_2 = 1.1 \frac{f_{cc}}{\sqrt{\varepsilon_{cu}}}. \tag{6}$$

$$f_0 = f_{co} - \frac{f_{co}}{f_{cc} - f_{co}}. \tag{7}$$

$$n_t = 6. \tag{8}$$

In these equations, E_1 and E_2 are the slopes of the first and second branch of the stress–strain curve, respectively. f_0 is the stress at which extension of the second branch of the curve intersects with the stress axis, and n_t is a parameter that controls the transition zone of the curve. f_c and ε_c represent stress and strain of confined concrete. These models were initially developed for AFRP-confined concrete columns, but further numerical evaluations showed this relation maintain very good accuracy for other types of FRP wraps. To prove this claim, a database of experimental results from previous researches was collected consisting of 340 test results of FRP confined concrete columns.[45–73] The summary of the variation range of effective parameters in the collected data are presented in Table A1 in Appendix A, in which letters A, C, and G denote aramid, carbon, and glass FRP, respectively.

It should be noted that there are many existing models available for prediction of the ultimate stress and strain of FRP-confined concrete. Ozbakkaloglu et al.[1] presented a comprehensive review of nearly 90 reported models at the time. Five more accurate and practical models were selected from those, which tabulated in Tables 1 and 2, and the proposed relations were used to calculate ultimate stress and strain for this database and the attained results were compared to the experimental results. To calculate the accuracy of the estimations, three different error measures of root mean square error, mean absolute error, and integral absolute error in addition to the coefficient of determination were used.[8] The obtained results are presented in Figures 1–4. Based on the presented results, the selected models in present study for the ultimate stress and strain of FRP-confined concrete performs better than the rest.

Another model that is required for determining the slenderness limit is the bilinear stress–strain curve. To assess the accuracy of the bilinear curve used in this study, experimental data from three previous research studies were considered.[70,71,79] Details of the utilized database of experimental results for the performance evaluation of the bilinear stress–strain curve are presented in Table A2 of Appendix A. The accuracy of the selected bilinear relation in this study (Equation (4) through Equation (8)) is compared to four other

TABLE 1 Strength models for circular confined concrete columns

No	Reference	Model
1	Lam and Teng[74]	$\frac{f_{cc}}{f_{co}} = 1 + 3.3 \frac{f_l}{f_{co}}$
2	Wang and Wu[66]	$\frac{f_{cc}}{f_{co}} = \frac{\left(1.0 + 5.54 \frac{f_l}{f_{co}}\right)}{\sqrt{1 + \frac{L-D}{353}\left(1 - 1.49 \frac{f_l}{f_{co}}\right)}}$
3	Wu and Zhou[75]	$\frac{f_{cc}}{f_{co}} = \frac{f_l}{f_{co}} + \sqrt{\left(\left(\frac{16.7}{f'^{0.42}_{co}} - \frac{f'^{0.42}_{co}}{16.7}\right)\frac{f_l}{f_{co}}\right) + 1}$
4	Pham and Hadi[76]	$\frac{f_{cc}}{f_{co}} = 0.91 + 1.88 \frac{f_l}{f_{co}} + 7.6 \frac{t_f}{d f_{co}}$
5	Djafar-Henni and Kassoul[77]	$\frac{f_{cc}}{f_{co}} = 1 + 1.2 \left(\frac{f_l}{f_{co}}\right)^{1.25} \left(\frac{k_l}{f_{co}}\right)^{0.37}$

TABLE 2 Strain models for circular confined concrete columns

No	Reference	Model
1	Djafar-Henni and Kassoul[77]	$\frac{\varepsilon_{cu}}{\varepsilon_{co}} = 2.3 + 1.2 \left(\frac{f_l}{f_{co}}\right)^{0.75} \left(\frac{\varepsilon_{hrup}}{\varepsilon_{co}}\right)^{1.25}$
2	Wu et al.[64]	$\frac{\varepsilon_{cu}}{\varepsilon_{co}} = 1 + 9.5 \frac{f_l}{f_{co}}$
3	Pham and Hadi[76]	$\frac{\varepsilon_{cu}}{\varepsilon_{co}} = 1 + 13.24 \frac{t_f E_f \varepsilon^2_{hrup}}{d f_{co} + 3.3 t_f E_f \varepsilon_{hrup}}$
4	Lam and Teng[74]	$\frac{\varepsilon_{cu}}{\varepsilon_{co}} = 1.75 + 12 \left(\frac{2 E_f t_f \varepsilon_{hrup}}{d f_{co}}\right) \left(\frac{\varepsilon_{hrup}}{\varepsilon_{co}}\right)^{0.45}$
5	Wei and Wu[78]	$\frac{\varepsilon_{cu}}{\varepsilon_{co}} = 1.75 + 12 \left(\frac{f_l}{f_{co}}\right)^{0.75} \left(\frac{f_{30}}{f_{co}}\right)^{0.62}$

models[51,64,77,80] using these experimental results. The attained results are demonstrated in Figure 5. As it can be seen, the relation used in this study provided the most accurate estimations in comparison to the other models.

Before proceeding to the next section, there is one important point that should be mentioned. Equation (4) is applicable for situations in which sufficient FRP confinement is provided for the column and accordingly the stress–strain curve of the column has an ascending second branch. It should be noted that the proposed slenderness limit in this study pertain to the sufficiently confined circular columns. This is due to the fact that the full confinement benefit of FRP wraps is used when the concrete is sufficiently confined and otherwise it is not economically and practically efficient. Accordingly, Equation (4) is chosen because of its acceptably higher accuracy in comparison to other existing counterparts. To determine whether a designed FRP confinement is sufficient or not, one can use the confinement efficiency threshold proposed by Arabshahi et al.:[8]
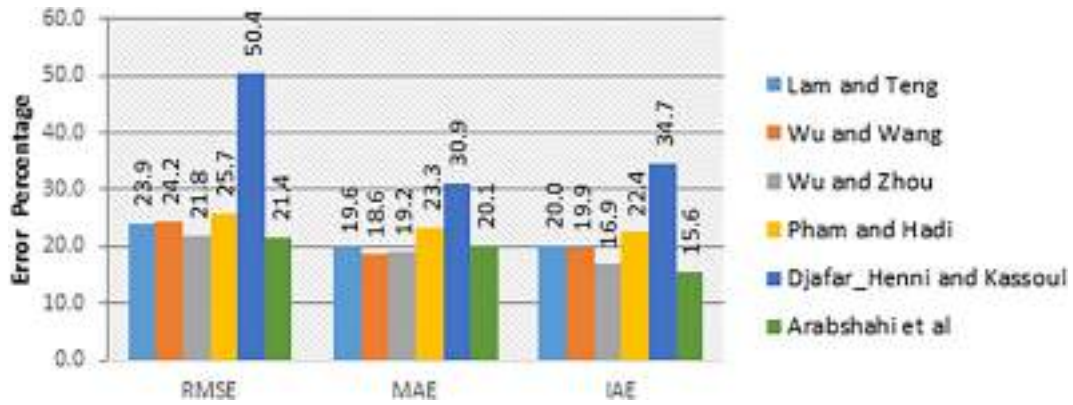
$$f_{l_{tr}} = 0.191 f_{co}. \tag{9}$$

FIGURE 1 Error percentage of the strength models for FRP-confined circular columns. FRP, fiber reinforced polymer
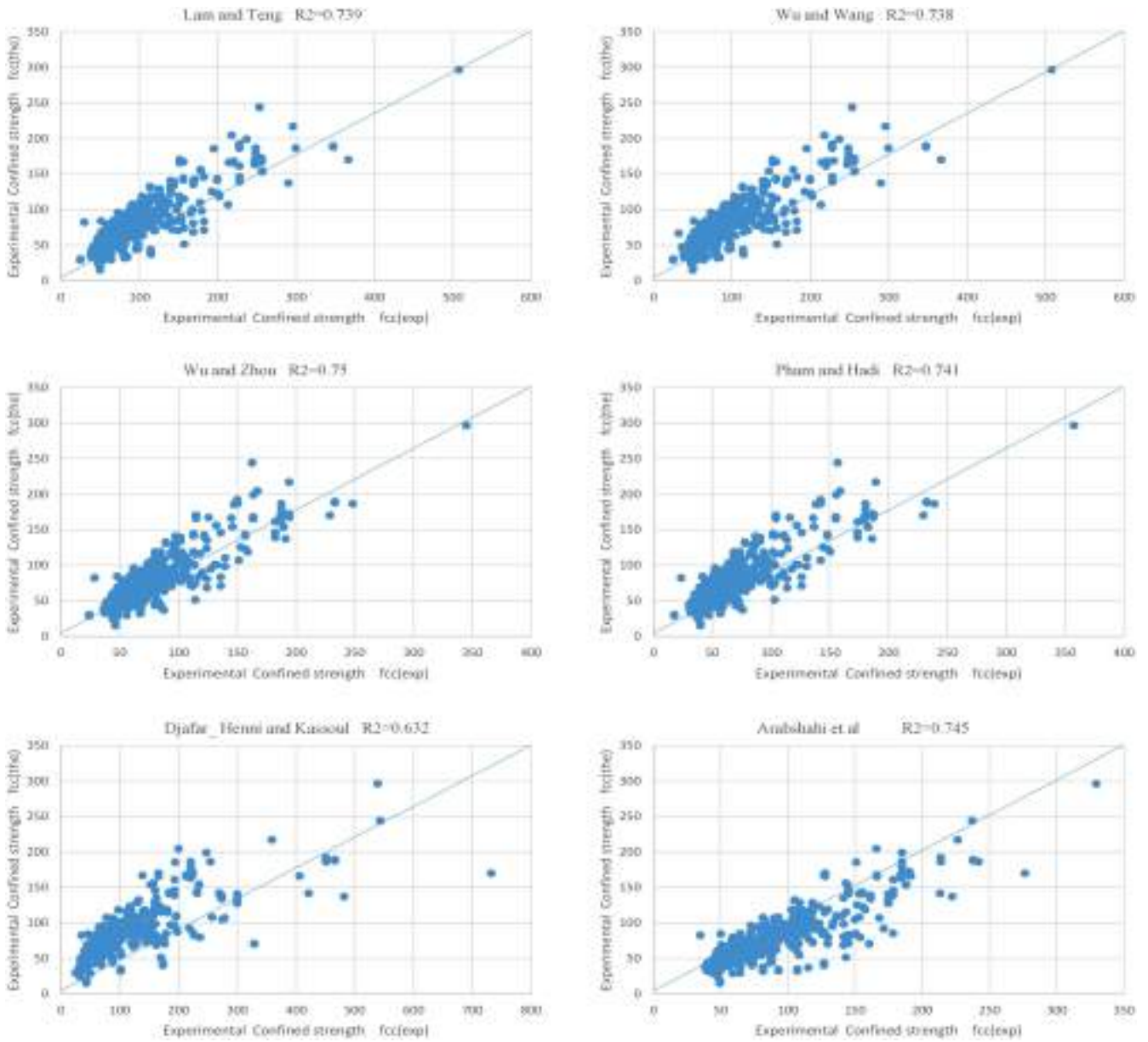

FIGURE 2 Performance of strength models for FRP-confined circular sections based on the experimental data. FRP, fiber reinforced polymer
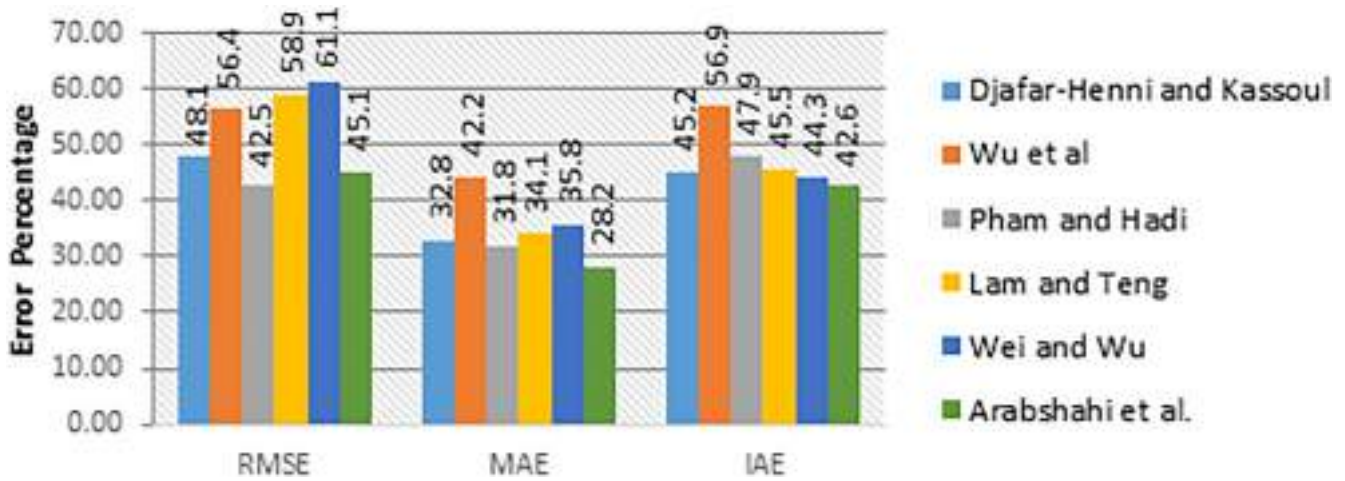
FIGURE 3 Error percentage of the strain models for FRP-confined circular columns. FRP, fiber reinforced polymer

3 | FORMULATION OF SLENDERNESS LIMIT

In this section, the slenderness limit for FRP-confined circular RC columns is derived analytically. The following relations are derived assuming the application of both steel and FRP reinforcing bars as well as hybrid FRP confinement. According to the definition of the slenderness limit, it is required that the compressive load carrying capacity of the column be equal to its buckling load in the critical slenderness value:

$$P_c = P_E. \tag{10}$$

In this equation, P_c is the compressive strength of the RC column and P_E is the Euler buckling load. The compressive strength for FRP-confined RC circular column is computed from the subsequent equation:

$$P_c = f_{cc}A_c + E_{sb}\varepsilon_{sb}A_{sb} + E_{fb}\varepsilon_{fb}A_{fb} + \sum_{i=1}^{n}E_{frp_i}\varepsilon_{cu}A_{frp_i}, \tag{11}$$

where f_{cc} and ε_{cu} are the ultimate stress and strain of confined concrete, respectively. These parameters are computed using Equations (1) and (2). E_{sb}, E_{fb}, and E_{frp_i} are the moduli of elasticity of the reinforcing steel bars and FRP bars and the ith type of confining FRP sheets with fibers in the longitudinal direction. It should be noted that FRP sheets with fibers in the longitudinal direction are used in some cases to improve flexural performance of concrete. However, in most cases only FRP wraps with fibers in the circumferential direction are used for strengthening concrete

columns. In such cases, the last term in Equation (11) is neglected.

Here ε_{sb} and ε_{fb} are the strains of steel and FRP rebars, respectively. Depending on the ultimate strain of confined concrete, the strain in steel bar at the critical slenderness is derived from the subsequent equation:

$$\varepsilon_{sb} = \begin{cases} \varepsilon_{cu} & \varepsilon_{cu} < \varepsilon_y \\ \varepsilon_y & \varepsilon_{cu} \geq \varepsilon_y \end{cases}. \tag{12}$$

Here, ε_y is the yield strain of steel. Note that the above relationship is used assuming the elastic-perfectly plastic material models for steel rebars. However, different material models including hardening effect can be used for reinforcing steel rebars.

In case of using FRP rebars, due to their brittle behavior, the strain in them is calculated from the next equation, in which ε_{uF} is the ultimate strain of FRP rebar in compression:

$$\varepsilon_{fb} = \begin{cases} \varepsilon_{cu} & \varepsilon_{cu} < \varepsilon_{uF} \\ 0 & \varepsilon_{cu} \geq \varepsilon_{uF} \end{cases}. \tag{13}$$

The cross-section area for different parts of the column were computed using the subsequent equations:

$$A_{sb} = n_{sb}\frac{\pi\phi_{sb}^2}{4}. \tag{14}$$

$$A_{fb} = n_{fb}\frac{\pi\phi_{fb}^2}{4}. \tag{15}$$
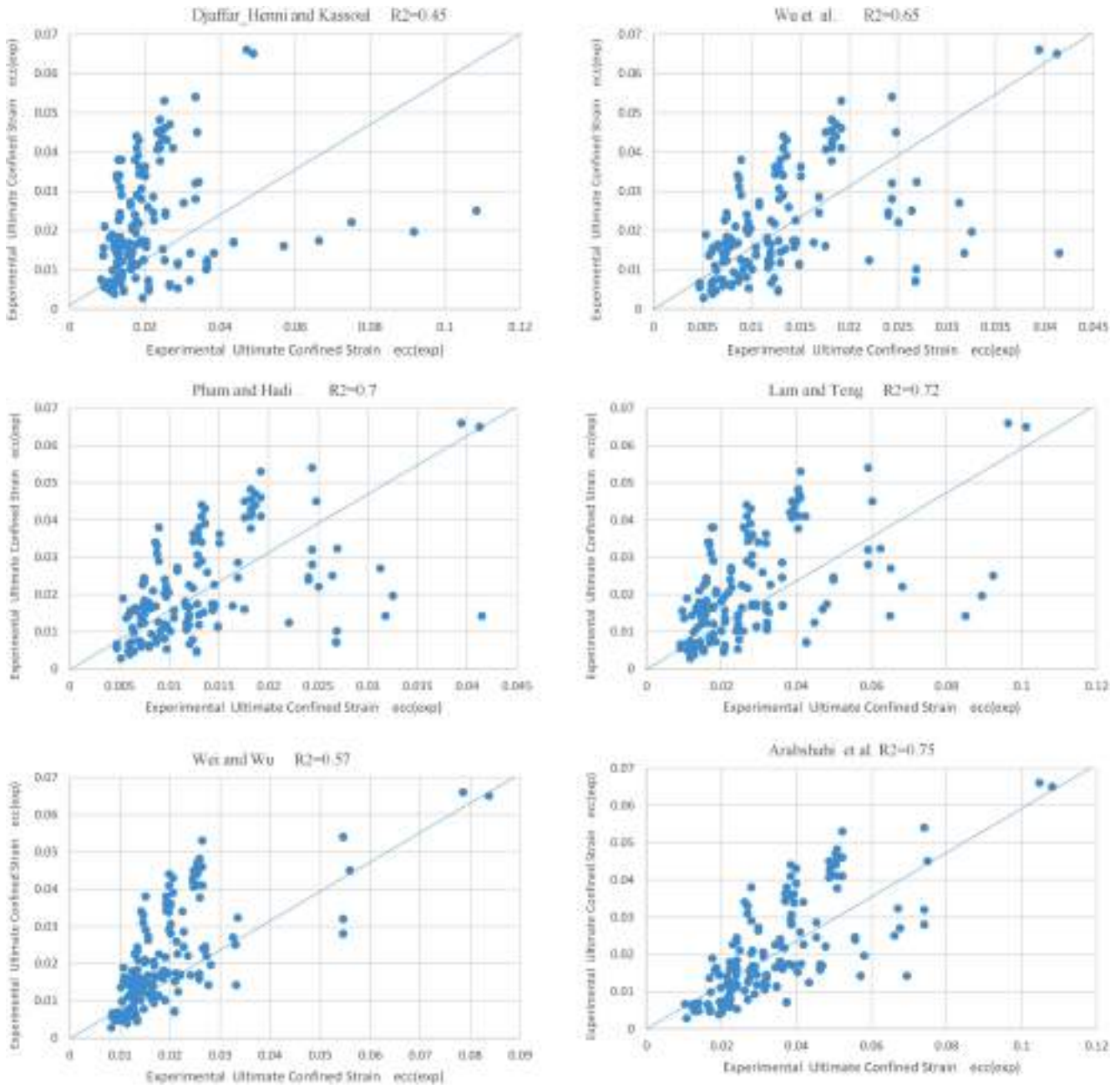
FIGURE 4 Performance of strain models for FRP-confined circular sections based on the experimental data. FRP, fiber reinforced polymer

$$A_{frp_i} = \pi d t_{fl_i}. \tag{16}$$

$$A_c = \frac{\pi \left(d^2 - n_{sb}\phi_{sb}^2 - n_{fb}\phi_{fb}^2 \right)}{4}. \tag{17}$$

In these equations, d, ϕ, n, and t_{fl} stand for column diameter, diameter, and number of reinforcing bars and thickness of FRP wrap in the longitudinal direction, respectively. While, the subscripts sb and fb indicate steel

and FRP bars, respectively. On the other side of the Equation (10), the Euler buckling load is derived from the succeeding well-known equation:

$$P_E = \frac{\pi^2 E_c I_{eff}}{(KL)^2}. \tag{18}$$

In this equality, L is the length of the column and K is the coefficient of effective buckling length. E_c is the
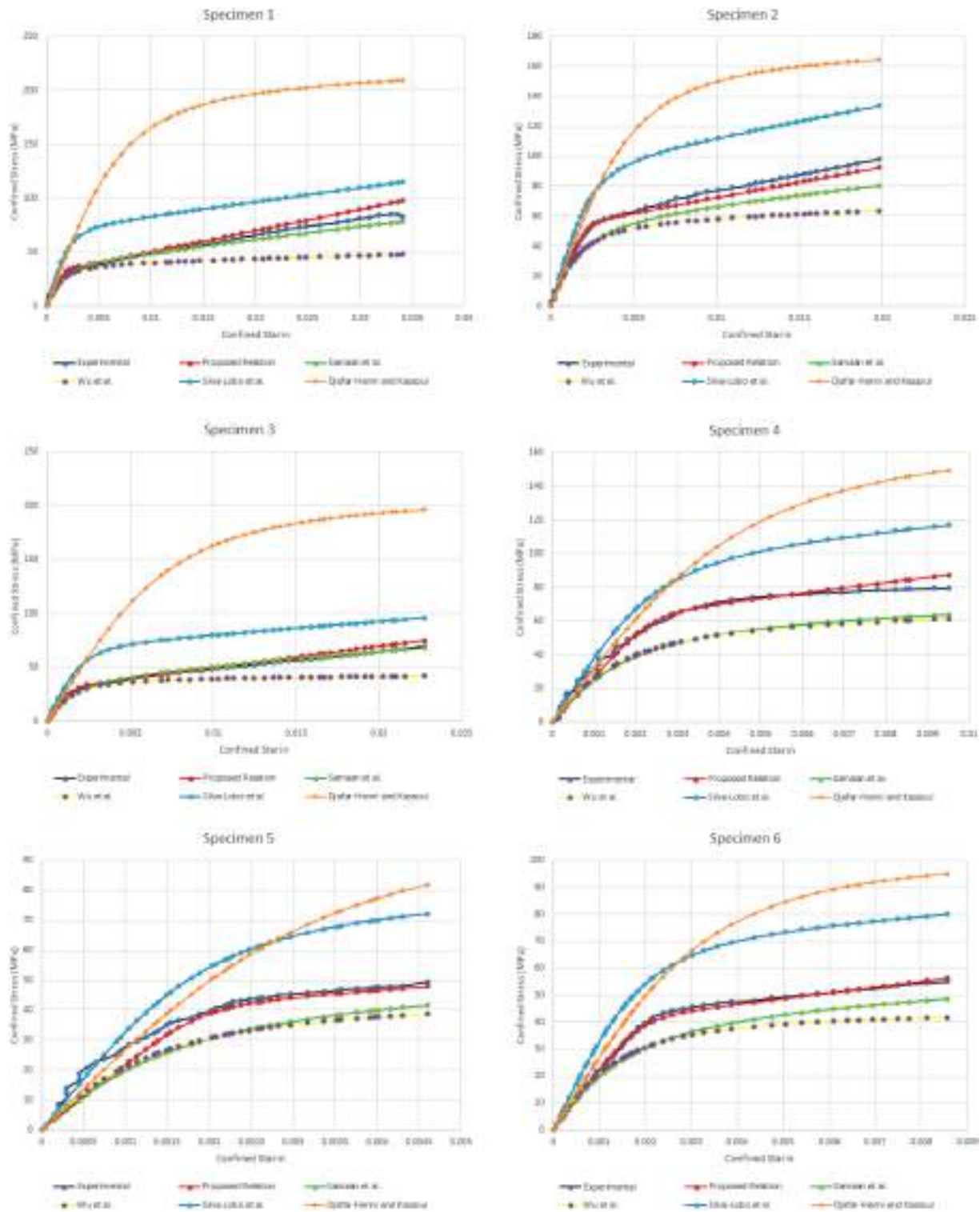
FIGURE 5 Comparison of experimental stress–strain curves with the model proposed by Arabshahi et al.[8]

concrete modulus of elasticity and I_{eff} is the effective flexural rigidity of the column which is computed using the following equation:

$$I_{eff} = \alpha\left(I_g + I'_b\right) + \beta I'_w, \qquad (19)$$

where I_g is the gross section moment of inertia and I'_b and I'_w are the equivalent moment of inertia due to reinforcing bars (steel or FRP) and FRP wraps, respectively:

$$I_g = \frac{\pi d^4}{64}. \qquad (20)$$

$$I'_b = I'_{sb} + I'_{fb} = \frac{\pi}{8}\left[\left(\frac{E_{sb}}{E_c} - 1\right)d_{sb}^3 t_{sb} + \left(\frac{E_{fb}}{E_c} - 1\right)d_{fb}^3 t_{fb}\right]. \tag{21}$$

$$I'_w = \sum_{i=1}^{n}\left(\frac{\pi}{8}\frac{E_{f_i}}{E_c}d^3 t_{fl_i}\right). \tag{22}$$

In Equation (21), d_{sb} and d_{fb} are the diameter of the equivalent smeared ring for longitudinal steel and FRP bars, respectively. Similarly, t_{sb} and t_{fb} are respectively thickness of equivalent smeared ring for steel and FRP bars. These parameters can be computed using the following equations:

$$d_{sb} = d - 2C_{sb} - \phi_{sb}, \tag{23}$$

$$d_{fb} = d - 2C_{fb} - \phi_{fb}, \tag{24}$$

$$t_{sb} = \frac{A_{sb}}{\pi d_{sb}}, \tag{25}$$

$$t_{fb} = \frac{A_{fb}}{\pi d_{fb}}, \tag{26}$$

where, C_{sb} and C_{fb} are the clear concrete cover to longitudinal reinforcing steel and FRP bars, respectively.

α and β in Equation (19), are the effective flexural rigidity coefficients for longitudinal reinforcement and FRP wraps, respectively. Previous studies proved that the flexural rigidity of RC section (or other composite sections) is not equal to the flexural rigidity of the equivalent cross-section.[81] Accordingly, various researchers have proposed different relations to predict the effective flexural rigidity of the RC beams and columns.[82,83] Avsar et al.[84] proposed the following relation for circular RC column with steel rebars:

$$\alpha = \begin{cases} 0.069 + 0.0032f_c + 0.876\dfrac{N}{f_cA_g} + 9.512\rho_s & \dfrac{N}{f_cA_g} > 0.26 - 1.75\rho_s \\[2ex] 0.239 - 0.0029f_c + 0.709\dfrac{N}{f_cA_g} + 12.809\rho_s & \dfrac{N}{f_cA_g} \le 0.26 - 1.75\rho_s \end{cases} \tag{27}$$

in these equations, N is the axial force applied to the column and ρ_s is the reinforcement ratio:

$$\rho_s = \frac{A_{sb}}{A_g}. \tag{28}$$

$$A_g = \frac{\pi d^2}{4}. \tag{29}$$

According to Avsar et al.[84] for values of $\frac{N}{f_cA_g}$ greater than 0.5, the coefficient of effective flexural rigidity approaches 0.75, and based on the definition of slenderness limit, that is the slenderness at which the buckling and ultimate axial capacity occurs at the same time, the ratio of $\frac{N}{f_cA_g}$ is surely higher than 0.5 (close to 1). Therefore, the value of 0.75 will be used in this study. On the other hand, the same reasoning can be used for FRP-confined concrete column. The fact is that there are very limited studies in this regard. In present study, the experimental results reported by Al-Nimry and Al-Rabadi[85] are adopted to estimate the coefficient β. Based on their observations, longitudinal FRP wraps increase flexural stiffness of FRP-confined RC columns significantly (more than doubled). Considering common FRP types and average cross-section area and reinforcement ratio for RC columns, it is calculated that this finding can be numerically justified by the application of a modification factor of $\beta = 0.20\tilde{\ }3$. Therefore, in the present study, the value of 0.25 is used and consequently, Equation (19) can be rewritten in the following form:

$$I_{eff} = 0.75\left(I_g + I'_b\right) + 0.25I'_w. \tag{30}$$

Now that all the necessary parameters for calculation of compressive strength and Euler buckling force are in hand, the slenderness limit can be derived by performing some mathematical operations on the expanded version of Equation (10):

$$\lambda_c = \frac{\pi}{r}\sqrt{\frac{E_cI_{eff}}{f_{cc}A_c + E_{sb}\varepsilon_{cu}A_{sb} + E_{fb}\varepsilon_{cu}A_{fb} + \sum_{i=1}^{n}E_{frp_i}\varepsilon_{cu}A_{frp_i}}}. \tag{31}$$

In this relation, r is the radius of gyration for the column cross-section:

$$r = \sqrt{\frac{I}{A}} = \sqrt{\frac{\frac{\pi d^4}{64}}{\frac{\pi d^2}{4}}} = \sqrt{\frac{d^2}{16}} = 0.25d. \tag{32}$$

Equation (31) is the critical slenderness limit for FRP-confined RC circular concrete columns. However, there is only one big question: which value should be used for the modulus of elasticity of concrete? To answer this question, one must return to the basics of the elasto-plastic buckling of columns. According to a classic and widely accepted theory, the utilization of reduced modulus of elasticity in the Equation (18) can

TABLE 3 Properties of experimental specimens used to assess the performance of the proposed slenderness limit

Specimen		Concrete prop.		Dimensions		Rebar prop.				FRP wrap prop.				Failure mode
No	Reference	f_{co} (MPa)	ε_{co} (%)	D (mm)	L (mm)	E_s (MPa)	$\varnothing$ (mm)	n	C_{sb} (mm)	E_{frp} (MPa)	f_{frp} (MPa)	t_{fc} (mm)	t_{fl} (mm)	
1	Tamuzs et al.[90]	25	0.16	150	1200	0	0	0	0	234,000	4500	0.34	0	Buckling
2		25	0.16	150	1500	0	0	0	0	234,000	4500	0.34	0	Buckling
3		25	0.16	150	2500	0	0	0	0	234,000	4500	0.34	0	Buckling
4		50	0.36	150	2500	0	0	0	0	234,000	4500	0.34	0	Buckling
5	Siddiqui et al.[33]	35.1	0.19	150	600	200,000	8	4	25	77,300	846	1	0	Buckling
6		35.1	0.19	150	600	200,000	8	4	25	77,300	846	1	2	Buckling
7		35.1	0.19	150	600	200,000	8	4	25	77,300	846	1	4	Buckling
8		35.1	0.19	150	900	200,000	8	4	25	77,300	846	1	0	Buckling
9		35.1	0.19	150	900	200,000	8	4	25	77,300	846	1	2	Buckling
10		35.1	0.19	150	900	200,000	8	4	25	77,300	846	1	4	Buckling
11		35.1	0.19	150	1200	200,000	8	4	25	77,300	846	1	0	Buckling
12		35.1	0.19	150	1200	200,000	8	4	25	77,300	846	1	2	Buckling
13		35.1	0.19	150	1200	200,000	8	4	25	77,300	846	1	4	Buckling
14	Wu et al.[63]	23.1	0.27	150	300	0	0	0	0	a	a	a	0	Comp. Fai.
15		23.1	0.27	150	300	0	0	0	0	a	a	a	0	Comp. Fai.
16		23.1	0.27	150	300	0	0	0	0	a	a	a	0	Comp. Fai.
17		23.1	0.27	150	300	0	0	0	0	a	a	a	0	Comp. Fai.
18		23.1	0.27	150	300	0	0	0	0	a	a	a	0	Comp. Fai.
19		23.1	0.27	150	300	0	0	0	0	a	a	a	0	Comp. Fai.
20		23.1	0.27	150	300	0	0	0	0	a	a	a	0	Comp. Fai.
21		23.1	0.27	150	300	0	0	0	0	a	a	a	0	Comp. Fai.
22		23.1	0.27	150	300	0	0	0	0	a	a	a	0	Comp. Fai.
23		23.1	0.27	150	300	0	0	0	0	a	a	a	0	Comp. Fai.
24		23.1	0.27	150	300	0	0	0	0	a	a	a	0	Comp. Fai.
25		23.1	0.27	150	300	0	0	0	0	a	a	a	0	Comp. Fai.
26		23.1	0.27	150	300	0	0	0	0	a	a	a	0	Comp. Fai.
27		23.1	0.27	150	300	0	0	0	0	a	a	a	0	Comp. Fai.
28		23.1	0.27	150	300	0	0	0	0	a	a	a	0	Comp. Fai.
29		23.1	0.27	150	300	0	0	0	0	a	a	a	0	Comp. Fai.
30		23.1	0.27	150	300	0	0	0	0	a	a	a	0	Comp. Fai.

TABLE 3 (Continued)

Specimen		Concrete prop.		Dimensions		Rebar prop.				FRP wrap prop.				Failure mode
No	Reference	f_{co} (MPa)	ε_{co} (%)	D (mm)	L (mm)	Ø (mm)	n	C_{sb} (mm)	E_s (MPa)	E_{frp} (MPa)	f_{frp} (MPa)	t_{fc} (mm)	t_{fl} (mm)	
31	Khorramian and Sadeghian[91]	30	0.21	260	3048	15	6	25	200,000	25,700	391	0.54	0	Buckling
32		30	0.21	260	3048	15	6	25	200,000	25,700/24600	391/4810	0.54	1.08	Buckling
33	Xing et al.[92]	48.8	0.24	300	1800	8	16	40	200,000	246,000	4810	0.668	0	Buckling

Abbreviations: Comp. Fai, compressive failure; FRP, fiber-reinforced polymer.
[a]Hybrid FRP confinement is used and the corresponding details are provided in Table 6

successfully predict the buckling load of columns.[86] The concept of reduced modulus of elasticity which takes into account the effect of unloading in the cross-section due to lateral deformation of the column at the buckling point was proposed by Considère.[87] Later, Von Karman[88] further substantiated this concept analytically and experimentally. The reduced modulus of elasticity for concrete is derived from the following equation:[86]

$$E_r = \left[\frac{1}{2} \left(\frac{1}{\sqrt{E_u}} + \frac{1}{\sqrt{E_t}} \right) \right]^{-2}. \tag{33}$$

In this equation, E_u is the tangential modulus of elasticity and stands for the unloading modulus. Assuming that no damage occurs in the concrete during the axial loading, the unloading modulus can be taken equal to the initial modulus of elasticity for confined concrete (i.e., $E_u = E_1$). However, such an assumption is not realistic and in the present study, based on the previous experimental works, a coefficient of 0.34 is applied on the initial modulus of elasticity to derive the unloading modulus.[89] E_t in this equation is also the tangential modulus of elasticity, that based on the definition of the slenderness limit, is equal to the tangential modulus at the failure point, that is, E_2. Therefore, the reduced modulus of elasticity for the confined concrete at the point of buckling is derived from the subsequent equation:

$$E_r = \left[\frac{1}{2} \left(\frac{1}{\sqrt{0.34E_1}} + \frac{1}{\sqrt{E_2}} \right) \right]^{-2}. \tag{34}$$

Although the results of the early experimental researches agree well with the predictions of reduced modulus buckling load, further investigations proved that columns can fail by buckling loads lower than the reduced modulus buckling load.[86] Therefore, a lower bound for buckling load is proposed, in which the tangential modulus of elasticity is used. Accordingly, the corresponding slenderness limit is also called the "tangential slenderness limit" in this study. Consequently, the following lower, λ_{ct}, and upper bound, λ_{cr}, are proposed for slenderness limit:

$$\lambda_{ct} = \frac{\pi}{r} \sqrt{\frac{E_2 I_{eff}}{f_{cc} A_c + E_{sb} \varepsilon_{cu} A_{sb} + + E_{fb} \varepsilon_{cu} A_{fb} + \sum_{i=1}^{n} E_{frp_i} \varepsilon_{cu} A_{frp_i}}}. \tag{35}$$

$$\lambda_{cr} = \frac{\pi}{r}\sqrt{\frac{E_r I_{eff}}{f_{cc}A_c + E_{sb}\varepsilon_{cu}A_{sb} + + E_{fb}\varepsilon_{cu}A_{fb} + \sum_{i=1}^{n} E_{frp_i}\varepsilon_{cu}A_{frp_i}}}. \tag{36}$$

It must be noted that in the derivation of each slenderness limit, in addition to the application of the corresponding modulus of elasticity in Equations (35) or (36), the relevant modulus of elasticity should also be used in the calculation of Equations (25) and (26) as well.

Since the real slenderness limit is between the values derived from Equations (35) and (36), and because for practical purposes, a single value is more desirable from the designer's standpoint, it is proposed that the average value of reduced and tangential slenderness limit be used. Needless to say, different combinations of these bounds may lead to different results, but further experimental investigations are required in this regard.

$$\lambda_{avg} = \frac{\lambda_{cr} + \lambda_{ct}}{2}. \tag{37}$$

4 | VERIFICATION OF THE PROPOSED MODEL

To verify the accuracy of the proposed model, a database of experimental results on short and slender columns, in which failure mode of the columns are reported by investigators, is collected. For this purpose, a set of 30 experiments from previous research studies were collected.[33,63,90–92] Table 3 presents the properties of these experiments and their corresponding failure modes. It should be noted that in some of these specimens, hybrid FRP confinement is used, while the properties of FRP wraps for them are listed in Table 4.

In addition to the proposed slenderness limit, some of the well-known existing relations for calculation of critical slenderness ratio are used for performance evaluations. These relations are introduced in Table 5. It should

TABLE 5 The existing relations for critical slenderness ratio

No.	Reference	Model
1	Hamdy et al.[93]	$\lambda_{cr} = \frac{\pi}{2.12}\sqrt{\frac{E_2}{f'_{cc}}}\sqrt{\frac{2\frac{E_u}{E_2}}{\frac{E_u}{E_2}+1}}$
2	Abdallah et al.[94]	$\lambda_{cr} = \pi\sqrt{\frac{E_2}{f'_{cc}}}\sqrt{\frac{E_2}{E_2+E_1}}$
3	Siddiqui et al.[33]	$\lambda_{cr} = 34\sqrt{\frac{f_{co}}{f'_{cc}}}$
4	Al-Salloum et al.[95]	$\lambda_{cr} = \pi\sqrt{\frac{E_c}{f'_{cc}}}$
5	Jiang and Teng-1[96]	$\lambda_{cr} = \frac{20f_{co}}{f'_{cc}}$
6	Jiang and Teng-2[96]	$\lambda_{cr} = \frac{20f_{co}}{f'_{cc}\left(1+\frac{0.06\varepsilon_{hrup}}{\varepsilon_{co}}\right)}$

TABLE 4 Properties of FRP wraps for specimens with hybrid confinement

Specimen		FRP properties in each layer								
No	Reference	$E_{frp}1$	$E_{frp}2$	$E_{frp}3$	$f_{frp}1$	$f_{frp}2$	$f_{frp}3$	$t_{f,hoop}1$	$t_{f,hoop}2$	$t_{f,hoop}3$
14	Wu et al.[63]	563,000	243,000	0	2543.5	4233.8	0	0.143	0.167	0.00
15		563,000	243,000	0	2543.5	4233.8	0	0.143	0.167	0.00
16		563,000	260,000	0	2543.5	4158.2	0	0.143	0.128	0.00
17		563,000	260,000	0	2543.5	4158.2	0	0.143	0.128	0.00
18		563,000	115,000	0	2543.5	2323.5	0	0.143	0.286	0.00
19		563,000	115,000	0	2543.5	2323.5	0	0.143	0.286	0.00
20		563,000	80,500	0	2543.5	1793.7	0	0.143	0.286	0.00
21		563,000	243,000	0	2543.5	4233.8	0	0.143	0.167	0.00
22		563,000	243,000	0	2543.5	4233.8	0	0.143	0.167	0.00
23		563,000	260,000	0	2543.5	4158.3	0	0.143	0.128	0.00
24		563,000	260,000	0	2543.5	4158.3	0	0.143	0.128	0.00
25		563,000	115,000	0	2543.5	2323.5	0	0.143	0.286	0.00
26		563,000	115,000	0	2543.5	2323.5	0	0.143	0.286	0.00
27		563,000	80,500	0	2543.5	1793.7	0	0.143	0.118	0.00
28		563,000	80,500	0	2543.5	1793.7	0	0.143	0.118	0.00
29		563,000	243,000	115,000	2543.5	4233.8	2323.5	0.143	0.167	0.286
30		563,000	243,000	115,000	2543.5	4233.8	2323.5	0.143	0.167	0.286

Abbreviation: FRP, FRP, fiber-reinforced polymer.

be noted that an example of using the proposed model for calculation of slenderness limit of a confined RC column (see Table B1) along with a calculation flowchart are presented in Appendix B (see Figure B1).

The predictions of proposed relations as well as the reviewed existing relations for the slenderness limit of FRP-confined RC circular columns are provided in Tables 6 and 7.

TABLE 6 The predicted slenderness limits for experimental specimens

Specimen		Existing slenderness	Proposed slenderness limit			Existing slenderness limit					
No	Reference	λ	λ_{ct}	λ_{cr}	λ_{avg}	Hamdy et al.	Abdallah et al.	Siddiqui et al.	Al-Salloum et al.	Jiang and Teng-1	Jiang and Teng-2
1	Tamuzs et al.[90]	32	5.98	9.56	7.77	4.47	6.83	19.28	54.60	6.43	4.02
2		40	5.98	9.56	7.77	4.47	6.83	19.28	54.60	6.43	4.02
3		67	5.98	9.56	7.77	4.47	6.83	19.28	54.60	6.43	4.02
4		67	6.89	11.49	9.19	5.21	7.91	33.03	78.68	18.87	14.91
5	Siddiqui et al.[33]	16	12.31	13.64	12.97	5.36	8.13	33.69	87.68	19.64	15.26
6		16	13.06	13.66	13.36	5.36	8.13	33.69	87.68	19.64	15.26
7		16	13.28	13.67	13.47	5.36	8.13	33.69	87.68	19.64	15.26
8		24	12.31	13.64	12.97	5.36	8.13	33.69	87.68	19.64	15.26
9		24	13.06	13.66	13.36	5.36	8.13	33.69	87.68	19.64	15.26
10		24	13.28	13.67	13.47	5.36	8.13	33.69	87.68	19.64	15.26
11		32	12.31	13.64	12.97	5.36	8.13	33.69	87.68	19.64	15.26
12		32	13.06	13.66	13.36	5.36	8.13	33.69	87.68	19.64	15.26
13		32	13.28	13.67	13.47	5.36	8.13	33.69	87.68	19.64	15.26
14	Wu et al.[63]	8	6.98	11.78	9.38	5.29	8.01	29.91	86.42	15.47	14.27
15		8	6.98	11.78	9.38	5.29	8.01	29.91	86.42	15.47	14.27
16		8	7.05	11.95	9.50	5.35	8.10	30.82	89.05	16.43	15.16
17		8	7.05	11.95	9.50	5.35	8.10	30.82	89.05	16.43	15.16
18		8	7.06	11.95	9.51	5.35	8.10	30.87	89.20	16.49	15.21
19		8	7.06	11.95	9.51	5.35	8.10	30.87	89.20	16.49	15.21
20		8	7.17	12.19	9.68	5.44	8.23	32.25	93.19	18.00	16.60
21		8	6.98	11.78	9.38	5.29	8.01	29.91	86.42	15.47	14.27
22		8	6.98	11.78	9.38	5.29	8.01	29.91	86.42	15.47	14.27
23		8	7.05	11.95	9.50	5.35	8.10	30.82	89.05	16.43	15.16
24		8	7.05	11.95	9.50	5.35	8.10	30.82	89.05	16.43	15.16
25		8	7.06	11.95	9.51	5.35	8.10	30.87	89.20	16.49	15.21
26		8	7.06	11.95	9.51	5.35	8.10	30.87	89.20	16.49	15.21
27		8	7.34	12.57	9.95	5.58	8.44	34.49	99.66	20.58	18.98
28		8	7.34	12.57	9.95	5.58	8.44	34.49	99.66	20.58	18.98
29		8	6.70	11.18	8.94	5.06	7.68	26.62	76.91	12.26	11.30
30		8	6.70	11.18	8.94	5.06	7.68	26.62	76.91	12.26	11.30
31	Khorramian and Sadeghian[91]	46.8	13.8	19.6	16.7	9.92	3.6	26.87	71.7	12.5	12.71
32		46.8	13.5	19.4	16.45	9.9	3.63	26.75	71	12.45	12.5
33	Xing et al.[92]	24	10.8	14.15	12.47	9.44	4.33	23.28	55.04	9.38	6.45

It is evident that the suggested slenderness limits provide very accurate estimations for most cases and the average slenderness limit can accurately predict the failure mode of all the collected experimental specimens.

5 | PARAMETRIC STUDY

Since different parameters are used as inputs for the proposed slenderness limit, it would be helpful for

TABLE 7 Predicted failure modes based on the calculated slenderness limits

Specimen		Observed failure mode	Proposed slenderness limit			Existing relations for slenderness limit					
No	Reference		λ_c	λ_r	λ_{avg}	Hamdy et al.	Abdallah et al.	Siddiqui et al.	Al-Salloum et al.	Jiang and Teng-1	Jiang and Teng-2
1	Tamuzs et al.[90]	Buckling	Bu	Bu	Bu	Bu	Bu	Bu	CF	Bu	Bu
2		Buckling	Bu	Bu	Bu	Bu	Bu	Bu	CF	Bu	Bu
3		Buckling	Bu	Bu	Bu	Bu	Bu	Bu	Bu	Bu	Bu
4		Buckling	Bu	Bu	Bu	Bu	Bu	Bu	CF	Bu	Bu
5	Siddiqui et al.[33]	Buckling	Bu	Bu	Bu	Bu	Bu	CF	CF	CF	Bu
6		Buckling	Bu	Bu	Bu	Bu	Bu	CF	CF	CF	Bu
7		Buckling	Bu	Bu	Bu	Bu	Bu	CF	CF	CF	Bu
8		Buckling	Bu	Bu	Bu	Bu	Bu	CF	CF	Bu	Bu
9		Buckling	Bu	Bu	Bu	Bu	Bu	CF	CF	Bu	Bu
10		Buckling	Bu	Bu	Bu	Bu	Bu	CF	CF	Bu	Bu
11		Buckling	Bu	Bu	Bu	Bu	Bu	CF	CF	Bu	Bu
12		Buckling	Bu	Bu	Bu	Bu	Bu	CF	CF	Bu	Bu
13		Buckling	Bu	Bu	Bu	Bu	Bu	CF	CF	Bu	Bu
14	Wu et al.[63]	Comp. Fai.	Bu	CF	CF	Bu	CF	CF	CF	CF	CF
15		Comp. Fai.	Bu	CF	CF	Bu	CF	CF	CF	CF	CF
16		Comp. Fai.	Bu	CF	CF	Bu	CF	CF	CF	CF	CF
17		Comp. Fai.	Bu	CF	CF	Bu	CF	CF	CF	CF	CF
18		Comp. Fai.	Bu	CF	CF	Bu	CF	CF	CF	CF	CF
19		Comp. Fai.	Bu	CF	CF	Bu	CF	CF	CF	CF	CF
20		Comp. Fai.	Bu	CF	CF	Bu	CF	CF	CF	CF	CF
21		Comp. Fai.	Bu	CF	CF	Bu	CF	CF	CF	CF	CF
22		Comp. Fai.	Bu	CF	CF	Bu	CF	CF	CF	CF	CF
23		Comp. Fai.	Bu	CF	CF	Bu	CF	CF	CF	CF	CF
24		Comp. Fai.	Bu	CF	CF	Bu	CF	CF	CF	CF	CF
25		Comp. Fai.	Bu	CF	CF	Bu	CF	CF	CF	CF	CF
26		Comp. Fai.	Bu	CF	CF	Bu	CF	CF	CF	CF	CF
27		Comp. Fai.	Bu	CF	CF	Bu	CF	CF	CF	CF	CF
28		Comp. Fai.	Bu	CF	CF	Bu	CF	CF	CF	CF	CF
29		Comp. Fai.	Bu	CF	CF	Bu	Bu	CF	CF	CF	CF
30		Comp. Fai.	Bu	CF	CF	Bu	Bu	CF	CF	CF	CF
31	Khorramian and Sadeghian[91]	Buckling	Bu	Bu	Bu	Bu	Bu	Bu	CF	Bu	Bu
32		Buckling	Bu	Bu	Bu	Bu	Bu	Bu	CF	Bu	Bu
33	Xing et al.[92]	Buckling	Bu	Bu	Bu	Bu	Bu	CF	CF	Bu	Bu

Abbreviations: Bu, buckling; CF, compressive failure.

designers to investigate the variation of the proposed slenderness limit versus the input parameters. For this purpose, the influence of five different parameters (namely concrete compressive strength, column diameter, FRP tensile strength, FRP wrap thickness, and longitudinal reinforcement ratio) on the variations of the slenderness limit will be studied. To achieve an understanding of the slenderness variations in practical cases, the effective parameters are varied in the ranges, which are usually used for columns in practical application. It is noteworthy that for the tensile strength of FRP, the variation range of typical FRP laminates suggested by ACI440-2R-17[28] and FIB-Bulletin-14[29] is used. These variation ranges for four of these parameters are listed in Table 8. It must be noted that since the proposed relation is applicable for columns with sufficient confinement, the number of circumferential FRP layers in the evaluations is selected such that to ensure sufficiency of FRP confinement.

In the following, the derived curves for variation of the slenderness limit versus different parameters are demonstrated.

Figure 6 represents the combined effect of concrete compressive strength and one of the other considered parameters on the slenderness limit, while the rest of the influential factors are kept constant.

To facilitate studying the interacting effect of the considered parameters, a two-dimensional version of these curves is presented in Figure 7. It is evident from these figures that increase in the concrete compressive strength results in increase in the slenderness limit. However, sensitivity of the slenderness limit to the concrete compressive strength at lower strengths is higher. It is also concluded from Figure 7 that for a constant concrete strength, increase in the strength, and thickness of FRP wrap reduces slenderness limit, while column diameter and reinforcement ratio have increasing effect. However, it is evident that the effect of reinforcement ratio on the slenderness limit at lower concrete strengths is negligible.

The next parameter is the column diameter, its effect on the slenderness limit is demonstrated in Figures 8 and 9. From these diagrams, it is concluded that increase in the column diameter will enhance the critical slenderness ratio for all case. Again, the inverse effect of FRP wrap strength and thickness on the slenderness limit is observed, while concrete compressive strength and reinforcement ratio have direct relation with the slenderness limit.
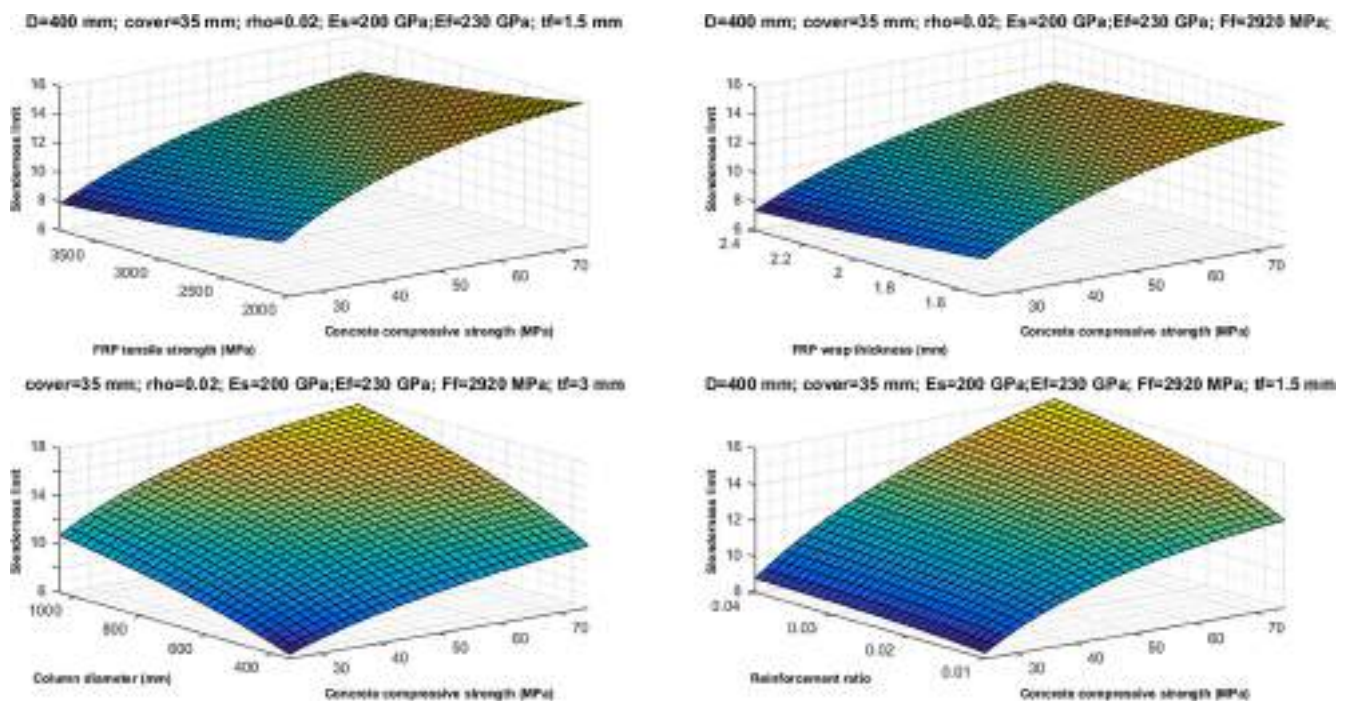
TABLE 8 The variation range of effective parameters in slenderness limit for practical columns

Parameter	Unit	Lower limit	Upper limit
f_c	MPa	25	75
F_{frp}	MPa	2050	3790
d	mm	350	1050
ρ_s	%	1	4

FIGURE 6 3D view of the slenderness limit variation versus concrete compressive strength
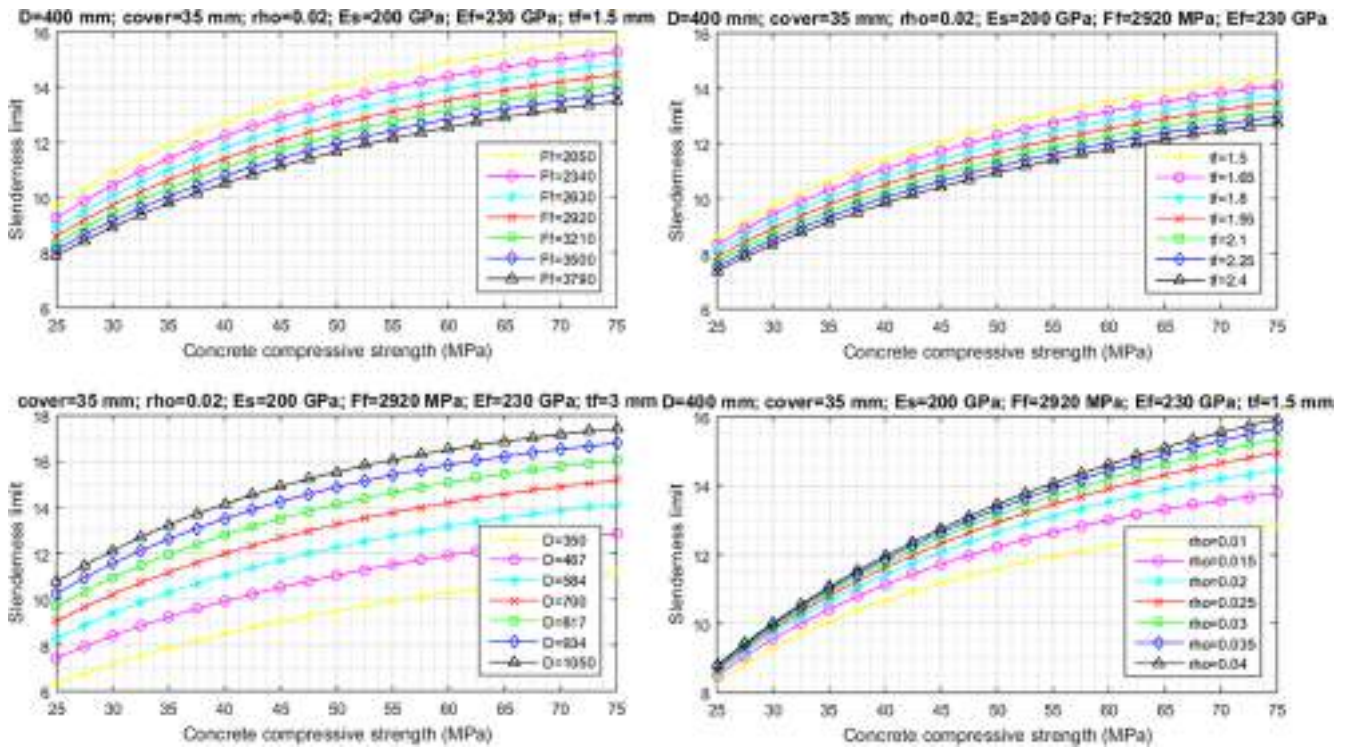
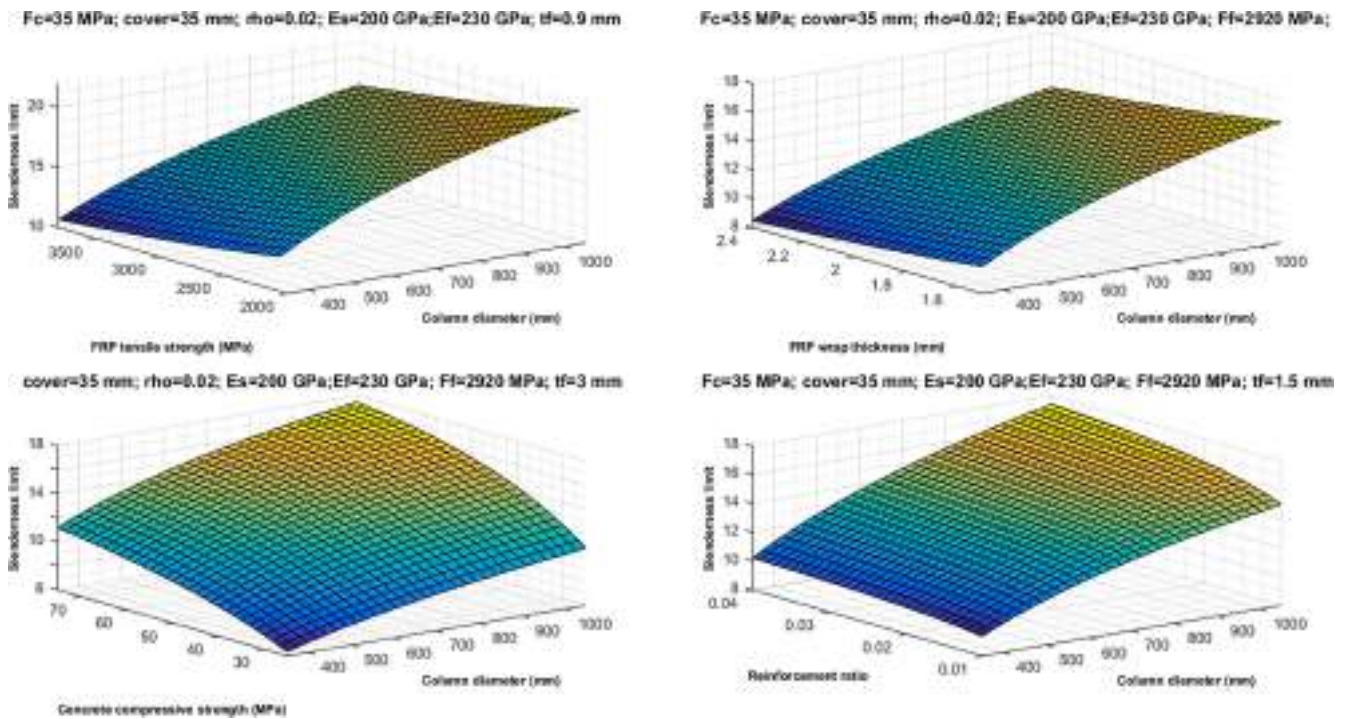**FIGURE 7** 2D view of the slenderness limit variation versus concrete compressive strength

FIGURE 8 3D view of the slenderness limit variation versus column diameter

In comparison with concrete compressive strength, the slenderness limit experiences a wider range of variation with change in the column diameter.

The influence of FRP tensile strength on the critical slenderness of FRP-confined RC column is demonstrated in Figures 10 and 11.
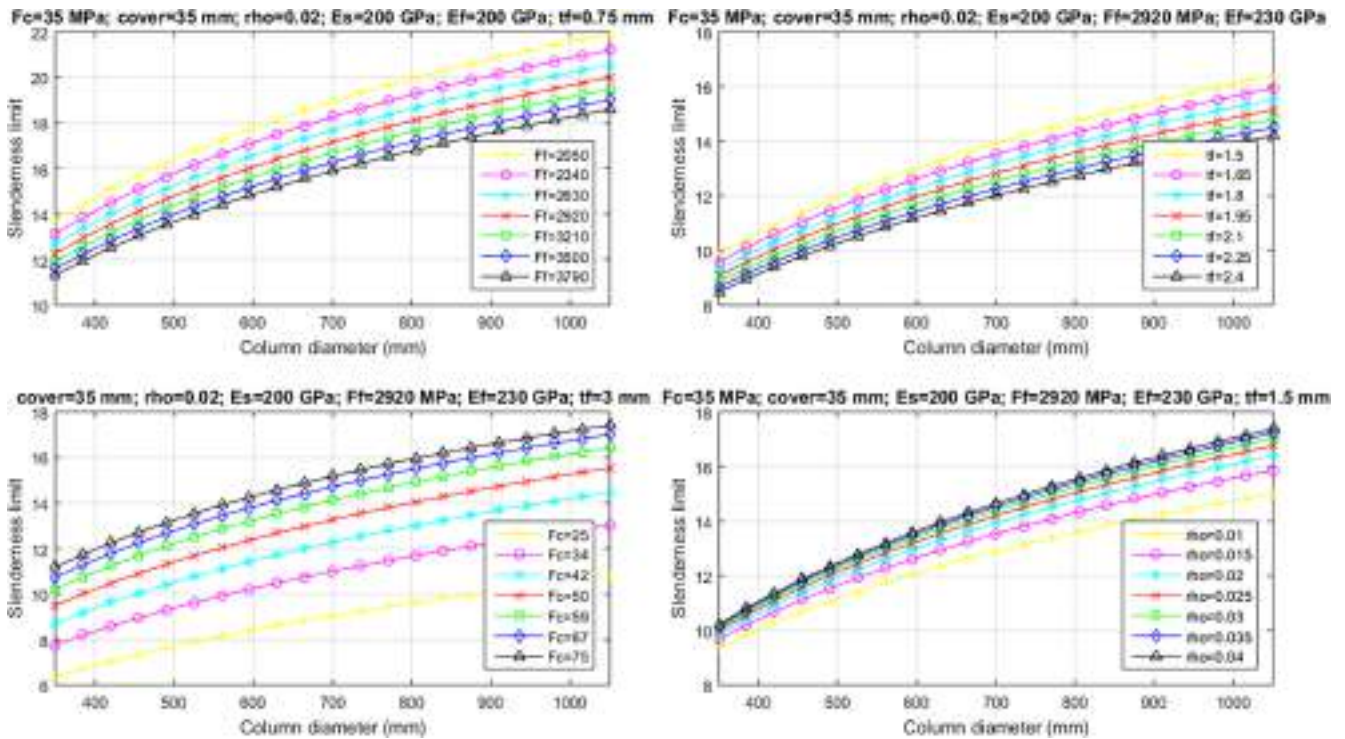
FIGURE 9 2D view of the slenderness limit variation versus column diameter
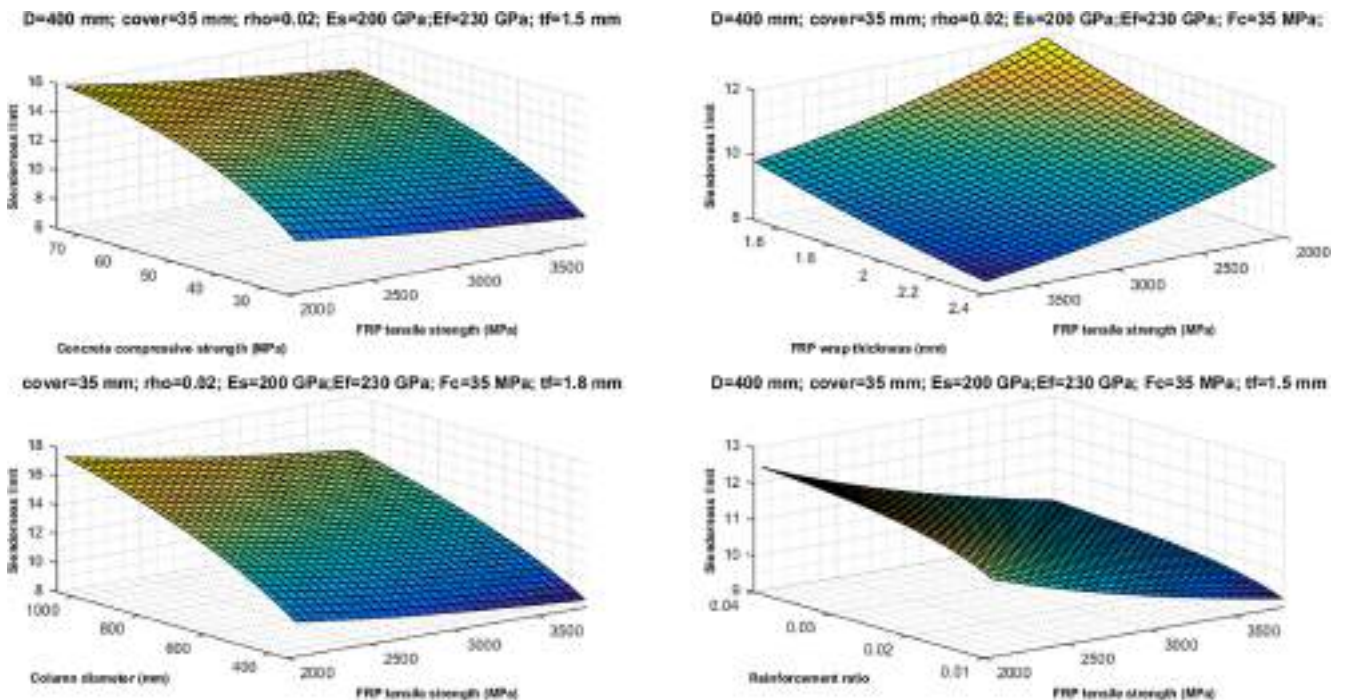
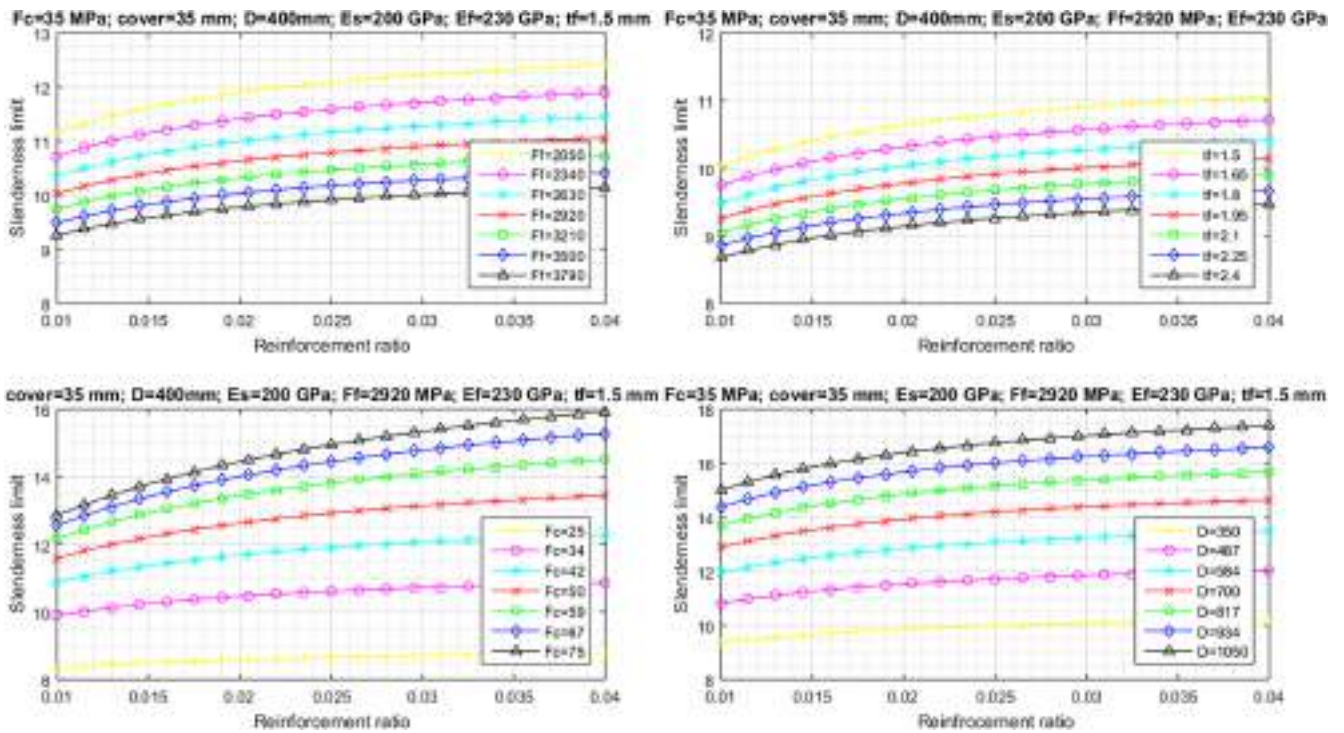**FIGURE 10** 3D view of the slenderness limit variation versus FRP tensile strength. FRP, fiber reinforced polymer

The reducing effect of FRP wrap strength on the slenderness limit, which was also noted in the previous diagrams, is evident in Figure 11. This reflects exactly what was discussed previously about the effect of confinement on the slenderness characteristics of a RC column. In other word, the confinement can reduce the critical slenderness of a RC column and if the reduced slenderness limit goes below the existing
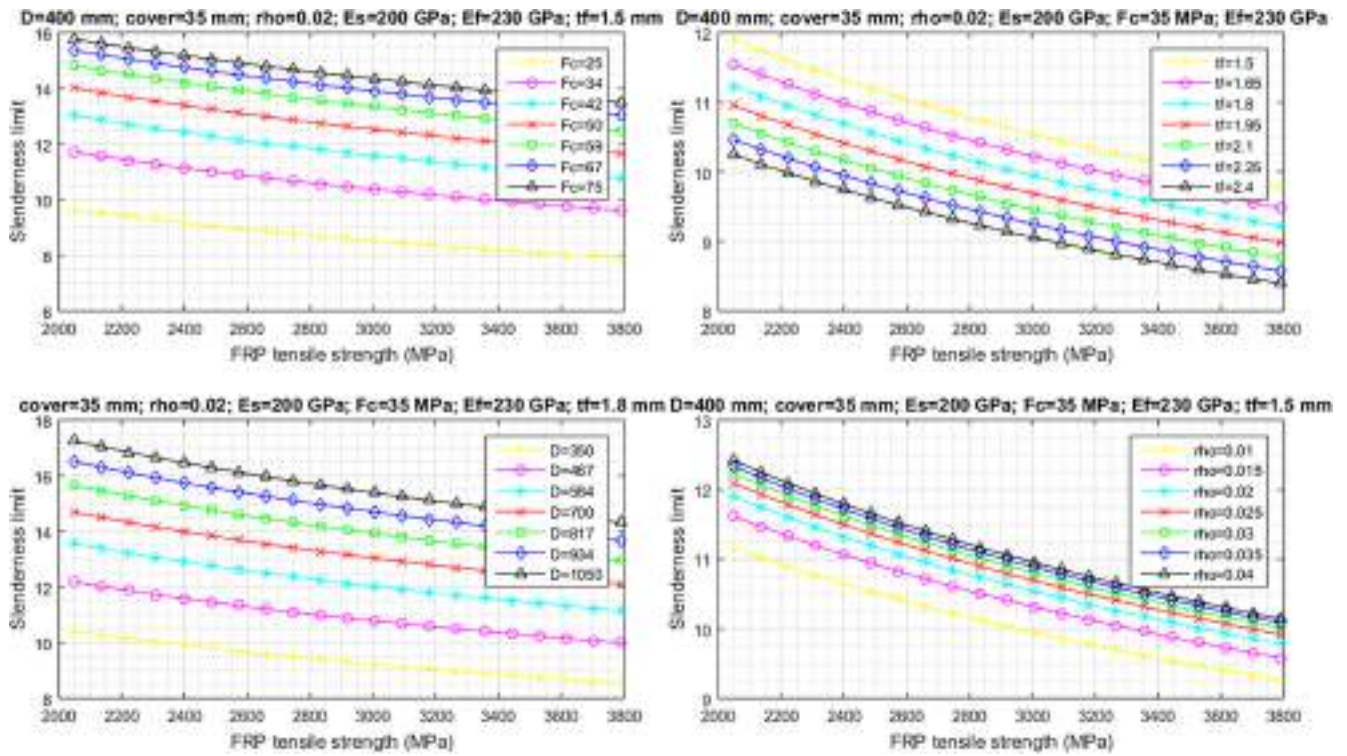
FIGURE 11   2D view of the slenderness limit variation versus FRP tensile strength. FRP, fiber reinforced polymer
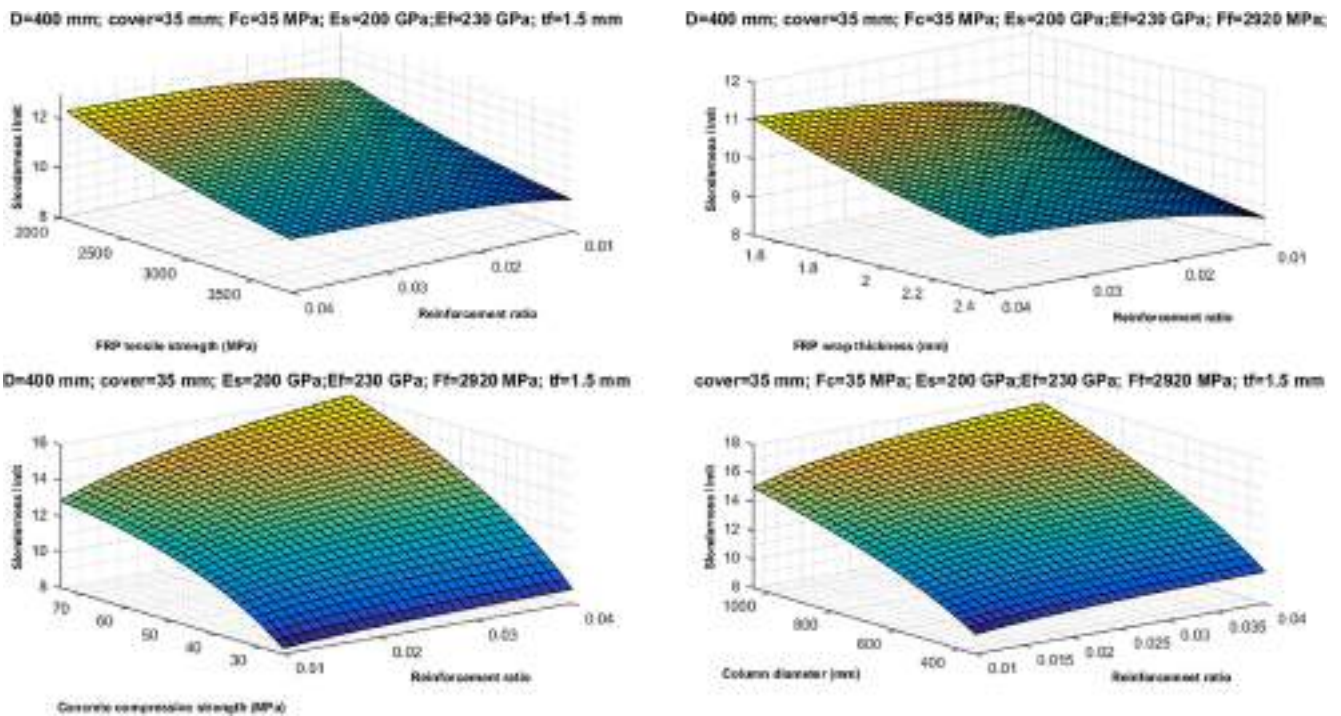
FIGURE 12   3D view of the slenderness limit variation versus reinforcement ratio

slenderness ratio of the column, it would become a slender column.

The next parameter, the reinforcement ratio, which it is evident from Figures 12 and 13 is not as effective as the other four parameters. The lower slope of the curves in Figure 12 proves this claim.

Finally, Figures 14 and 15 demonstrate variation of the slenderness limit with FRP wrap thickness. Based on these

FIGURE 13 2D view of the slenderness limit variation versus reinforcement ratio
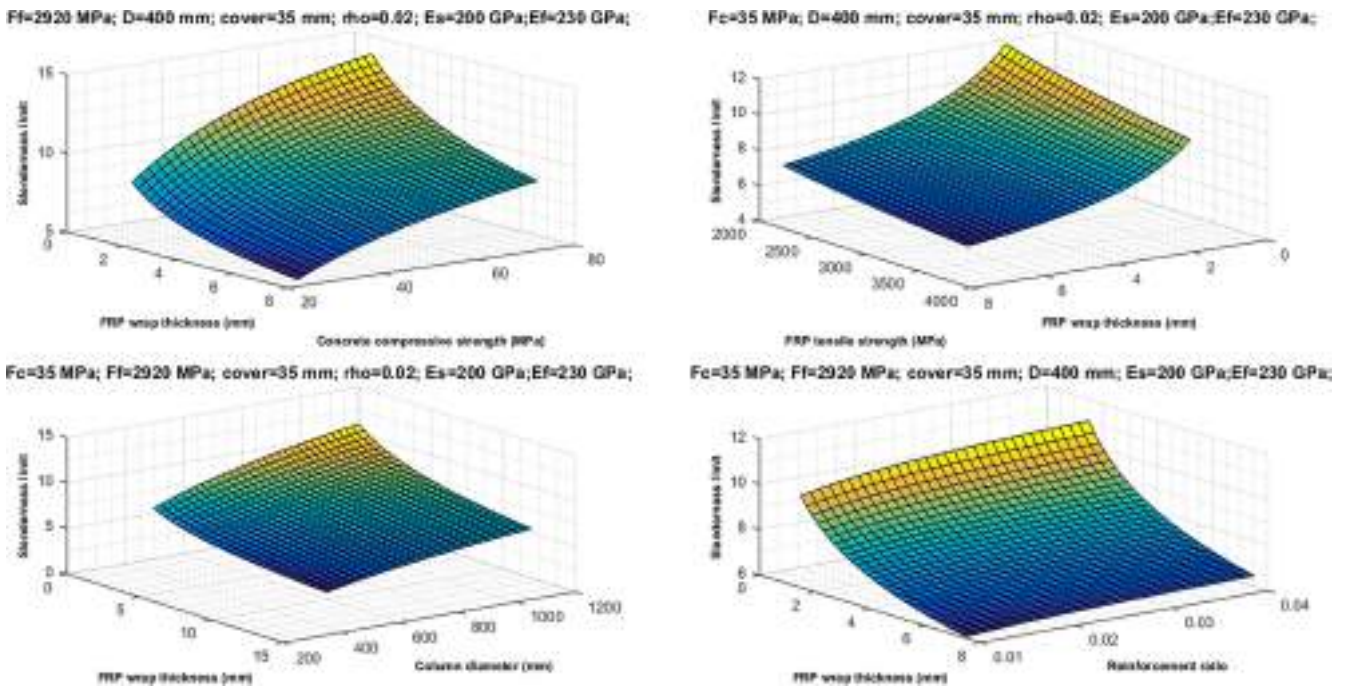
FIGURE 14 3D view of the slenderness limit variation versus FRP thickness variation. FRP, fiber reinforced polymer

diagrams, increase in the thickness of FRP wrap reduces the slenderness limit for the sample specimens. This is because the fact that increase in the FRP thickness increases the confinement pressure and therefore increases the concrete compressive strength. Based on the definition of slenderness limit, increase in the concrete compressive strength reduces the slenderness limit, at which the compressive failure and buckling occur simultaneously.
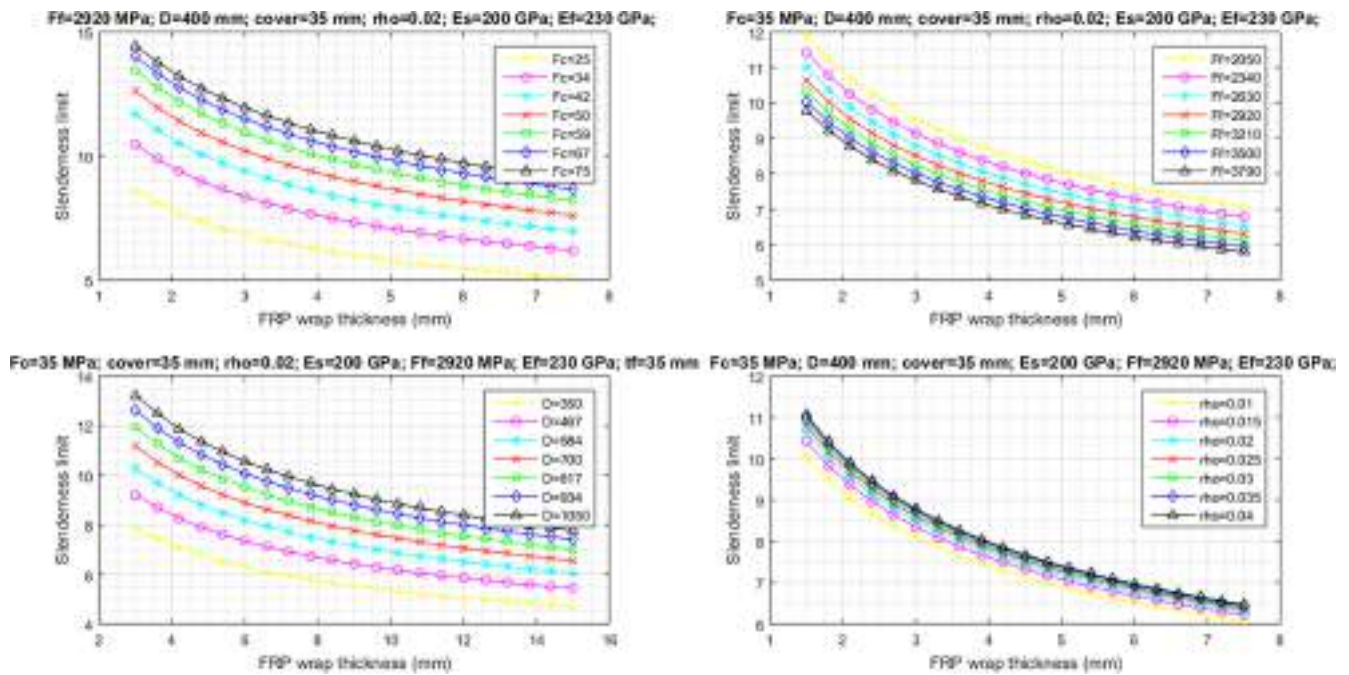
FIGURE 15 2D view of the slenderness limit variation versus FRP thickness variation. FRP, fiber reinforced polymer

Based on the performed evaluations, it is concluded that the values for the proposed slenderness limit of typical FRP-confined RC columns varied between 8 and 24. The higher values are fairly close to the slenderness limit suggested by design codes such as ACI318-17[97] for unconfined RC columns of 22. Since there is no suggestion for the slenderness of FRP-confined RC columns in the current design codes, one may decide to use the value suggested for unconfined RC columns in existing design codes. However, such decision would not be very reasonable. Because by using such value, there is a high probability that many confined columns with a smaller slenderness ratio to be considered as a short column and therefore unattainable load carrying capacity would be assigned to them. This conclusion proves the importance of revising the current design code requirements and introducing the slenderness limit of FRP-confined RC columns.

6 | CONCLUSION

In this paper, using the mechanic-based relationships of short and slender circular FRP-confined RC columns, a new relationship was proposed to determine the slenderness limit. In the derivation process of the proposed limit, a new and highly accurate model for behavior of confined concrete was utilized. The developed relation incorporates the effect of FRP confinement as well as hybrid longitudinal reinforcement. The only limitation of that is considered in derivation of the proposed relation is the assumption of sufficient FRP confinement that guarantees a bilinear stress–strain curve with ascending second branch for the confined concrete. A comparison of the attained results using the proposed relation with experimental data collected from the literature demonstrates the high accuracy of the prediction made. Moreover, it was shown that the suggested model is more accurate than some of the existing relations. To demonstrate the effect of different parameters on the value of the slenderness limit in practical ranges of variations, a parametric study was performed that showed the extent of influence of each parameter on the slenderness limit of FRP-confined RC columns. Finally, it was reported that the slenderness limit values for typical columns vary between 8 and 24. Considering the fact that there is no available code-approved slenderness limit for FRP-confined RC columns and on the other hand the value proposed by most of the design codes for unconfined RC columns is about 22, using this value for the evaluation and design of FRP confined RC column is not logical. Therefore, there is an urgent need to a code-approved slenderness limit for FRP-confined RC columns, and the proposed relation is this study can be considered for this purpose. However, further experimental evaluations are required.

CONFLICT OF INTEREST

The authors declare that they have no conflict of interest.

DATA AVAILABILITY STATEMENT

The data that support the findings of this study are available from the corresponding author upon reasonable request.

ORCID

Mohammadreza Tavakkolizadeh https://orcid.org/0000-0002-0932-4605

REFERENCES

1. Ozbakkaloglu T, Lim JC, Vincent T. FRP-confined concrete in circular sections: review and assessment of stress–strain models. Eng Struct. 2013;49:1068–88.

2. Ziaadiny H, Abbasnia R. Unified cyclic stress-strain model for FRP-confined concrete circular, square and rectangular prisms. Struct Concr. 2016;17:220–34.

3. Siddiqui N, Abbas H, Almusallam T, Binyahya A, Al-Salloum Y. Compression behavior of FRP-strengthened RC square columns of varying slenderness ratios under eccentric loading. J Build Eng. 2020;32:101512.

4. Saadatmanesh H, Ehsani MR, Li MW. Strength and ductility of concrete columns externally reinforced with fiber composite straps. ACI Struct J. 1994;91:434–47.

5. Arabshahi A, Gharaei-Moghaddam N, Tavakkolizadeh M. Proposition of new applicable strength models for concrete columns confined with fiber reinforced polymers. SN Appl Sci. 2019;1:1677.

6. Fanaradelli T, Rousakis T. Assessment of analytical stress and strain at peak and at ultimate conditions for fiber-reinforcement polymer-confined reinforced concrete columns of rectangular sections under axial cyclic loading. Struct Concr. 2020;1–14.

7. Saljoughian A, Mostofinejad D. Using grooving and corner strip-batten techniques for seismic strengthening of square reinforced concrete columns with fiber-reinforced polymer composites. Struct Concr. 2020;21:2066–82.

8. Arabshahi A, Gharaei-Moghaddam N, Tavakkolizadeh M. Development of applicable design models for concrete columns confined with aramid fiber reinforced polymer using multi-expression programming. Structure. 2020;23:225–44.

9. Chellapandian M, Prakash SS, Sharma A. Experimental investigations on hybrid strengthening of short reinforced concrete column elements under eccentric compression. Struct Concr. 2019;20:1955–73.

10. Arabshahi, A., Gharaei Moghaddam, N. and Tavakkolizadeh, M., 2015. A new strength model for FRP confined circular concrete columns. Presented at: Third Conference on Smart Monitoring, Assessment and Rehabilitation of Civil Structures, Antalya, Turkey.

11. Wang J, Lu S, Yang J. Behavior of eccentrically loaded rectangular RC columns wrapped with CFRP jackets under different preloading levels. J Build Eng. 2021;34:101943.

12. Mai AD, Sheikh MN, Yamakado K, Hadi MN. Nonuniform CFRP wrapping to prevent sudden failure of FRP Confined Square RC columns. J Compos Constr. 2020;24:04020063.

13. Yang J, Lu S, Wang J, Wang Z. Behavior of CFRP partially wrapped square seawater sea-sand concrete columns under axial compression. Eng Struct. 2020;222:111119.

14. Mai AD, Sheikh MN, Hadi MN. Investigation on the behaviour of partial wrapping in comparison with full wrapping of square RC columns under different loading conditions. Constr Build Mater. 2018;168:153–68.

15. Pham TM, Hadi MN, Youssef J. Optimized FRP wrapping schemes for circular concrete columns under axial compression. J Compos Constr. 2015;19:04015015.

16. Ali AH, Mohamed HM, Chalioris CE, Deifalla A. Evaluating the shear design equations of FRP-reinforced concrete beams without shear reinforcement. Eng Struct. 2021;235:112017.

17. Sabzi J, Esfahani MR, Ozbakkaloglu T, Farahi B. Effect of concrete strength and longitudinal reinforcement arrangement on the performance of reinforced concrete beams strengthened using EBR and EBROG methods. Eng Struct. 2020;205:110072.

18. Mai AD, Sheikh MN, Hadi MN. Strain model for discretely FRP confined concrete based on energy balance principle. Eng Struct. 2021;241:112489.

19. Zhou JK, Lin G, Teng JG. Stress-strain behavior of FRP-confined concrete containing recycled concrete lumps. Constr Build Mater. 2021;267:120915.

20. Lin G, Teng JG. Advanced stress-strain model for FRP-confined concrete in square columns. Compos Part B Eng. 2020;197:108149.

21. Lai MH, Song W, Ou XL, Chen MT, Wang Q, Ho JCM. A path dependent stress-strain model for concrete-filled-steel-tube column. Eng Struct. 2020;211:110312.

22. Dong CX, Kwan AKH, Ho JCM. A constitutive model for predicting the lateral strain of confined concrete. Eng Struct. 2015;91:155–66.

23. Kwan AKH, Dong CX, Ho JCM. Axial and lateral stress–strain model for FRP confined concrete. Eng Struct. 2015;99:285–95.

24. Lai MH, Griffith AM, Hanzic L, Wang Q, Ho JCM. Interdependence of passing ability, dilatancy and wet packing density of concrete. Constr Build Mater. 2021;270:121440.

25. Lai MH, Binhowimal SAM, Griffith AM, Hanzic L, Chen Z, Wang Q, et al. Shrinkage, cementitious paste volume, and wet packing density of concrete. Struct Concr. 2020.

26. Lai MH, Liang YW, Wang Q, Ren FM, Chen MT, Ho JCM. A stress-path dependent stress-strain model for FRP-confined concrete. Eng Struct. 2020;203:109824.

27. Ho JCM, Ou XL, Chen MT, Wang Q, Lai MH. A path dependent constitutive model for CFFT column. Eng Struct. 2020; 210:110367.

28. ACI Committee 440. Guide for the design and construction of externally bonded FRP systems for strengthening concrete structures (ACI 440.2 R-17). Farmington Hills, MI: American Concrete Institute; 2017.

29. fib Bulletins. Externally bonded FRP reinforcement for RC structures (fib Bulletin No. 14). Lausanne, Switzerland; International Federation for Structural Concrete (fib); 2001.

30. CSA. Design and construction of building components with fiber reinforced polymers (CSA-S806-02, R2007). Toronto, Canada: Canadian Standards Association; 2002.

31. Pan JL, Xu T, Hu ZJ. Experimental investigation of load carrying capacity of the slender reinforced concrete columns wrapped with FRP. Constr Build Mater. 2007;21:1991–6.

32. Jiang T, Teng JG. Theoretical model for slender FRP-confined circular RC columns. Constr Build Mater. 2012;32:66–76.

33. Siddiqui NA, Alsayed SH, Al-Salloum YA, Iqbal RA, Abbas H. Experimental investigation of slender circular RC columns

strengthened with FRP composites. Constr Build Mater. 2014; 69:323–34.

34. Karimi K, Tait MJ, El-Dakhakhni WW. Analytical modeling and axial load design of a novel FRP-encased steel–concrete composite column for various slenderness ratios. Eng Struct. 2013;46:526–34.

35. Ali O. Structural reliability of biaxial loaded short/slender-square FRP-confined RC columns. Constr Build Mater. 2017; 151:370–82.

36. Hales TA, Pantelides CP, Reaveley LD. Analytical buckling model for slender FRP-reinforced concrete columns. Compos Struct. 2017;176:33–42.

37. Al-Nimry H, Soman A. On the slenderness and FRP confinement of eccentrically-loaded circular RC columns. Eng Struct. 2018;164:92–108.

38. Gajdošová K, Bilčík J. Slender reinforced concrete columns strengthened with fibre reinforced polymers. Slovak J Civil Eng. 2011;19:27–31.

39. Punurai W, Hsu CTT, Punurai S, Chen J. Biaxially loaded RC slender columns strengthened by CFRP composite fabrics. Eng Struct. 2013;46:311–21.

40. Jiang T, Teng JG. Behavior and design of slender FRP-confined circular RC columns. J Compos Constr. 2012;17:443–53.

41. Gajdosova K, Bilcik J. Full-scale testing of CFRP-strengthened slender reinforced concrete columns. J Compos Constr. 2013; 17:239–48.

42. Leite L, Bonet JL, Pallarés L, Miguel PF, Fernández-Prada MA. Experimental research on high strength concrete slender columns subjected to compression and uniaxial bending with unequal eccentricities at the ends. Eng Struct. 2013;48:220–32.

43. Pallarés L, Bonet JL, Miguel PF, Prada MF. Experimental research on high strength concrete slender columns subjected to compression and biaxial bending forces. Eng Struct. 2008;30: 1879–94.

44. Richard RM, Abbott BJ. Versatile elastic-plastic stress-strain formula. J Eng Mech Div. 1975;101:511–5.

45. Kshirsagar S, Lopez-Anido RA, Gupta RK. Environmental aging of fiber-reinforced polymer-wrapped concrete cylinders. Mater J. 2000;97:703–12.

46. Pessiki S, Harries KA, Kestner JT, Sause R, Ricles JM. Axial behavior of reinforced concrete columns confined with FRP jackets. J Compos Constr. 2001;5:237–45.

47. Xiao Y, Wu H. Compressive behavior of concrete confined by carbon fiber composite jackets. J Mater Civil Eng. 2000;12:139–46.

48. Mirmiran A, Shahawy M, Samaan M, Echary HE, Mastrapa JC, Pico O. Effect of column parameters on FRP-confined concrete. J Compos Constr. 1998;2:175–85.

49. Ahmad SH, Khaloot AR, Irshaid A. Behaviour of concrete spirally confined by fibreglass filaments. Mag Concr Res. 1991;43:143–8.

50. Nanni A, Bradford NM. FRP jacketed concrete under uniaxial compression. Constr Build Mater. 1995;9:115–24.

51. Samaan M, Mirmiran A, Shahawy M. Model of concrete confined by fiber composites. J Struct Eng. 1998;124:1025–31.

52. De Lorenzis L, Tepfers R. Applicability of FRP confinement to strengthen concrete columns. Nordic Conc Res Publ. 2004;31: 64–72.

53. Aire, C., Gettu, R. and Casas, J.R., 2001. Study of the compressive behavior of concrete confined by fiber reinforced composites carbon, 1.

54. Lin CT, Li YF. An effective peak stress formula for concrete confined with carbon fiber reinforced plastics. Can J Civil Eng. 2003;30:882–9.

55. Liang M, Wu ZM, Ueda T, Zheng JJ, Akogbe R. Experiment and modeling on axial behavior of carbon fiber reinforced polymer confined concrete cylinders with different sizes. J Reinf Plast Compos. 2012;31:389–403.

56. Chastre C, Silva MA. Monotonic axial behavior and modelling of RC circular columns confined with CFRP. Eng Struct. 2010; 32:2268–77.

57. Kumutha R, Vijai K, Palanichamy M. Analytical models for FRP confined circular concrete columns. Mater Sci. 2012;13(4): 489–97.

58. Ilki A, Peker O, Karamuk E, Demir C, Kumbasar N. FRP retrofit of low and medium strength circular and rectangular reinforced concrete columns. J Mater Civil Eng. 2008;20:169–88.

59. Matthys S, Toutanji H, Audenaert K, Taerwe L. Axial load behavior of large-scale columns confined with fiber-reinforced polymer composites. ACI Struct J. 2005;102:258.

60. Faella, C., Realfonzo, R. and Salerno, N., Sulla resistenza e deformazione di elementi in ca confinati con tessuti in FRP. Presented at: Proceedings of the Atti dell'XI Congresso Nazionale "L'ingegneria sismica in Italia", Genova, Italy 2004 25-29).

61. Lam L, Teng JG. Ultimate condition of fiber reinforced polymer-confined concrete. J Compos Constr. 2004;8:539–48.

62. Mandal S, Hoskin A, Fam A. Influence of concrete strength on confinement effectiveness of fiber-reinforced polymer circular jackets. ACI Struct J. 2005;102:383.

63. Wu G, Wu ZS, Lu ZT, Ando YB. Structural performance of concrete confined with hybrid FRP composites. J Reinf Plast Compos. 2008;27:1323–48.

64. Wu HL, Wang YF, Yu L, Li XR. Experimental and computational studies on high-strength concrete circular columns confined by aramid fiber-reinforced polymer sheets. J Compos Constr. 2009;13:125–34.

65. Lim JC, Ozbakkaloglu T. Investigation of the influence of the application path of confining pressure: tests on actively confined and FRP-confined concretes. J Struct Eng. 2015;141: 04014203.

66. Wang YF, Wu HL. Size effect of concrete short columns confined with aramid FRP jackets. J Compos Constr. 2010;15:535–44.

67. Lim JC, Ozbakkaloglu T. Influence of silica fume on stress–strain behavior of FRP-confined HSC. Constr Build Mater. 2014;63:11–24.

68. Ozbakkaloglu T, Akin E. Behavior of FRP-confined normal- and high-strength concrete under cyclic axial compression. J Compos Constr. 2012;16:451–63.

69. Almusallam TH. Behavior of normal and high-strength concrete cylinders confined with E-glass/epoxy composite laminates. Compos Part B Eng. 2007;38:629–39.

70. Wang LM, Wu YF. Effect of corner radius on the performance of CFRP-confined square concrete columns: test. Eng Struct. 2008;30:493–505.

71. Benzaid R, Mesbah H, Chikh NE. FRP-confined concrete cylinders: axial compression experiments and strength model. J Reinf Plast Compos. 2010;29:2469–88.

72. Akogbe RK, Liang M, Wu ZM. Size effect of axial compressive strength of CFRP confined concrete cylinders. Int J Concr Struct Mater. 2011;5:49–55.

73. Jiang C, Wu YF, Jiang JF. Effect of aggregate size on stress-strain behavior of concrete confined by fiber composites. Compos Struct. 2017;168:851–62.

74. Lam L, Teng J. Design-oriented stress–strain model for FRP-confined concrete. Constr Build Mater. 2003;17:471–89.

75. Wu YF, Zhou YW. Unified strength model based on Hoek-Brown failure criterion for circular and square concrete columns confined by FRP. J Compos Constr. 2010;14:175–84.

76. Pham TM, Hadi MN. Confinement model for FRP confined normal-and high-strength concrete circular columns. Constr Build Mater. 2014;69:83–90.

77. Djafar-Henni I, Kassoul A. Stress–strain model of confined concrete with aramid FRP wraps. Constr Build Mater. 2018;186:1016–30.

78. Wei YY, Wu YF. Unified stress–strain model of concrete for FRP-confined columns. Constr Build Mater. 2012;26:381–92.

79. Karabinis AI, Rousakis TC. Concrete confined by FRP material: a plasticity approach. Eng Struct. 2002;24:923–32.

80. Lobo PS, Faustino P, Jesus M, Marreiros R. Design model of concrete for circular columns confined with AFRP. Compos Struct. 2018;200:69–78.

81. Mirza S. Flexural stiffness of rectangular reinforced concrete columns. ACI Struct J. 1990;87:425–35.

82. Mehanny SS, Kuramoto H, Deierlein GG. Stiffness modeling of reinforced concrete beam-columns for frame analysis. Struct J. 2001;98:215–25.

83. Khuntia M, Ghosh SK. Flexural stiffness of reinforced concrete columns and beams: analytical approach. Struct J. 2004;101:351–63.

84. Avşar Ö, Bayhan B, Yakut A. Effective flexural rigidities for ordinary reinforced concrete columns and beams. Struct Design Tall Spec Build. 2014;23:463–82.

85. Al-Nimry HS, Al-Rabadi RA. Axial–flexural interaction in FRP-wrapped RC columns. Int J Concr Struct Mater. 2019;13:53.

86. Bažant ZP, Cedolin L. Stability of structures: elastic, inelastic, fracture, and damage theories. Singapore: World Scientific Publishing Co.; 2003.

87. Considère, A., 1891. Résistance des pièces comprimées. Presented at: Annexe au Compte Rendu du Congrès International des Procédés de Construction. Paris.

88. von Kármán T. Untersuchungen über knickfestigkeit. Mitteilungen über Forschungsarbeiten auf dem Gebiete des Ingenieurwesens insbesondere aus den Laboratorien der technischen Hochschulen. Berlin, Heidelberg: Springer; 1910. p. 1–44.

89. Lam L, Teng JG, Cheung CH, Xiao Y. FRP-confined concrete under axial cyclic compression. Cem Concr Compos. 2006;28:949–58.

90. Tamuzs V, Tepfers R, Zile E, Valdmanis V. Stability of round concrete columns confined by composite wrappings. Mech Compos Mater. 2007;43:445–52.

91. Khorramian K, Sadeghian P. Hybrid system of longitudinal CFRP laminates and GFRP wraps for strengthening of existing circular concrete columns. Eng Struct. 2021;235:112028.

92. Xing L, Lin G, Chen JF. Behavior of FRP-confined circular RC columns under eccentric compression. J Compos Constr. 2020;24:04020030.

93. Mohamed HM, Abdel-Baky HM, Masmoudi R. Nonlinear stability analysis of concrete-filled fiber-reinforced polymer-tube columns: experimental and theoretical investigation. ACI Struct J. 2010;107:699–708.

94. Abdallah MH, Mohamed HM, Masmoudi R. Experimental assessment and theoretical evaluation of axial behavior of short and slender CFFT columns reinforced with steel and CFRP bars. Constr Build Mater. 2018;181:535–50.

95. Al-Salloum YA, Al-Amri GS, Siddiqui NA, Almusallam TH, Abbas H. Effectiveness of CFRP strengthening in improving cyclic compression response of slender RC columns. J Compos Constr. 2018;22:04018009.

96. Jiang T, Teng JG. Slenderness limit for short FRP-confined circular RC columns. J Compos Constr. 2012;16:650–61.

97. ACI Committee 318. Building code requirements for structural concrete (ACI 318–19) and commentary. Farmington Hills, MI: American Concrete Institute; 2019.

AUTHOR BIOGRAPHIES

Alireza Arabshahi, PhD Candidate, Civil Engineering Department, Ferdowsi University of Mashhad, Mashhad, Iran. Email: alireza.arabshahi@mail.um.ac.ir.

Mohammadreza Tavakkolizadeh, Assistant Professor, Civil Engineering Department, Ferdowsi University of Mashhad, Iran. Email: drt@um.ac.ir.

APPENDIX A: Experimental database for verification of confined concrete models

TABLE A1 Summary of the collected experimental results

No	Reference	Fiber type	Concrete properties		Diameter	FRP properties			Stress and strain	
			f_{co} (MPa)	ε_{co} (%)	D (mm)	f_{frp} (MPa)	E_{frp} (MPa)	t_{frp} (mm)	ε_{cu} (%)	f_{cc} (MPa)
1–3	Kshirsagar et al.[45]	G	38–39.5	0.22–0.23	102	363	19,900	1.42	1.6–1.73	57–63.1
4–7	Pessiki et al.[46]	G	26–33	0.2–0.22	152–508	330–580	19,100–38,100	1–3	0.88–1.94	33.5–52.5
8–33	Xiao and Wu[47]	C	33.7–55.2	0.22–0.27	152	1577	10,500	0.38–1.14	0.37–1.66	47.9–106.5
34–60	Mirmiran et al.[48]	G	29.8–31.2	0.21–0.22	153	565	19,185	0.61–3.07	N.R	33.7–91.9
61–69	Ahmad et al.[49]	G	38.99–62.24	0.23–0.27	101.6	2070	48,300	0.88	0.33–1.24	51.61–145.6
70–100	Nanni and Bradford[50]	G–A	35.6–46.6	0.22–0.24	150	283–1150	52,000–62,200	0.3–4.3	0.6–5.433	41.2–118.87
101–109	Samaan et a1.[51]	G	29.7–31.7	0.21–0.22	305	524–641	37,233–40,749	1.44–2.97	3.17–4.69	55.1–96.1
110–113	De lorenzis and Tepfers[52]	C	38–43	0.23–0.24	120	1028	91,100	0.3–0.45	0.95–1.35	58.5–67.3
114–129	Aire et al.[53]	G–C	30–60	0.24–0.26	150	3000–3900	65,000–240,000	0.117–1.788	0.28–3.23	41–170
130–156	Lin and Li[54]	C	17.2–27.5	0.19–0.21	100–150	4240	236,000	0.11–0.33	N.R	37.89–107.4
157–169	Liang et al.[55]	C	22.7–25.9	0.21–0.24	100–300	3591	242,000	0.167–0.501	1.93–2.48	60.10–69.10
170–182	Chastre and Silva[56]	C	35.2–38	0.22–0.23	150–250	3339–3937	226,000–241,000	0.176–0.704	0.99–2.25	56.36–107.76
183–195	Kumutha et al.[57]	G	24.13	0.2	150	150–250	11,000–19,500	1–2.20	N.R	36.10–47.44
196–209	Ilki et al.[58]	C	9.88–23.44	0.18–0.20	250	3430	230,000	0.165–0.825	2.2–4.5	29.07–95.05
210–206	Matthys et al.[59]	G–C	34.3–39.3	0.22–0.23	400	780–2600	60,000–198,000	0.6–1.2	0.43–1.2	33.20–55.30
207–216	Faella et al.[60]	C	21.1–28.04	0.2–0.21	150	4500	240,000	0.17–0.34	1.33–2.76	51.80–90.96
217–234	Lam and Teng[61]	C–G	34.3–38.5	0.22–0.23	152	450–3420	22,460–230,000	0.165–2.54	1.02–2.52	51.90–97.30
235–249	Mandal et al.[62]	C–G	31–81	0.22–0.27	100	575–784	26,100–47,000	1.3–2.6	0.32–3.08	54.50–102.70
250–252	Wu et al.[63]	A	23.1	0.27	150	2323.5	115,000	0.286	0.23	45.20–53.70
253–244	Wu et al.[64]	A	46.43–101.18	0.26–0.46	100	2060	118,000	0.286–0.858	0.63–1.88	78.29–204.51
245–235	Lim and Ozbakkaloglu[65]	A	51.6–128	0.25–0.38	63	2390	128,500	0.2–0.4	1.65–4.64	103.30–170.3
236–253	Wang and Wu[66]	A	28.79–50.64	0.2–0.24	70–194	2060	118,000	0.0572–0.572	0.33–1.15	44.20–107.5
254–265	Lim and Ozbakkaloglu[67]	A	85.7–120.9	0.31–0.36	152.5	2600	118,200	1.2	1.74–2.18	165.2–178.5
266–277	Ozbakkaloglu and Akin[68]	A	39–106	0.21–0.35	152.5	2900	120,000	0.4–1.2	1.45–3.11	67.1–154.7
278–279	Al-mussallam[69]	G	40–100	0.23–0.33	150	540	27,000	1.3–3.9	0.32–2.72	55.5–125.2
280–295	Wang and Wu[70]	C	29.2–52.3	0.23–0.25	150	3482–3500	230,500–230,000	0.165–0.33	1.17–3.57	53.8–103
296–311	Benzaid et al.[71]	C	29.51–63.01	0.17–0.38	160	4300	238,000	0.13–0.39	2.52–22.01	49.9–100.4
312–320	Akogbe et al.[72]	C	25.2–28.1	0.21–0.38	100–300	3248	242,000	0.167–0.501	1.80–2.79	58.8–66.4
321–340	Jiang et al.[73]	C	28.38–38.58	0.199–0.237	150	3400	230,000	0.167–0.501	1.59–3.62	51.47–132.48

Abbreviations: FRP, FRP, fiber-reinforced polymer; NR, not reported.

TABLE A2 Properties of experimental specimens used to assess the accuracy of the bilinear curve model

No	Reference	Concrete properties		Specimen dimensions		FRP properties			Confined concrete properties		
		f_{co} (MPa)	ε_{co} (%)	d (mm)	L (mm)	f_f (MPa)	E_f (MPa)	t_f (mm)	ε_{hrup} (%)	f_{cc} (MPa)	ε_{cu} (%)
1	Wang and Wu[70]	30.9	0.19	150	300	3482	230,500	0.33	1.24	84.4	3.45
2		52.1	0.21	150	300	3500	230,000	0.33	1.23	99.3	1.90
3	Benzaid et al.[71]	29.51	0.377	160	320	4300	238,000	0.39	1.49	71.4	22.98
4		58.24	0.302	160	320	4300	238,000	0.13	1.45	77.5	8.36
5	Karabinis and Rousakis[79]	38.5	2.8	200	320	4400	240,000	0.234	1.50	51.5	8.77
6		38.5	2.8	200	320	4400	240,000	0.234	1.50	50.0	5.77

Abbreviation: FRP, FRP, fiber-reinforced polymer.

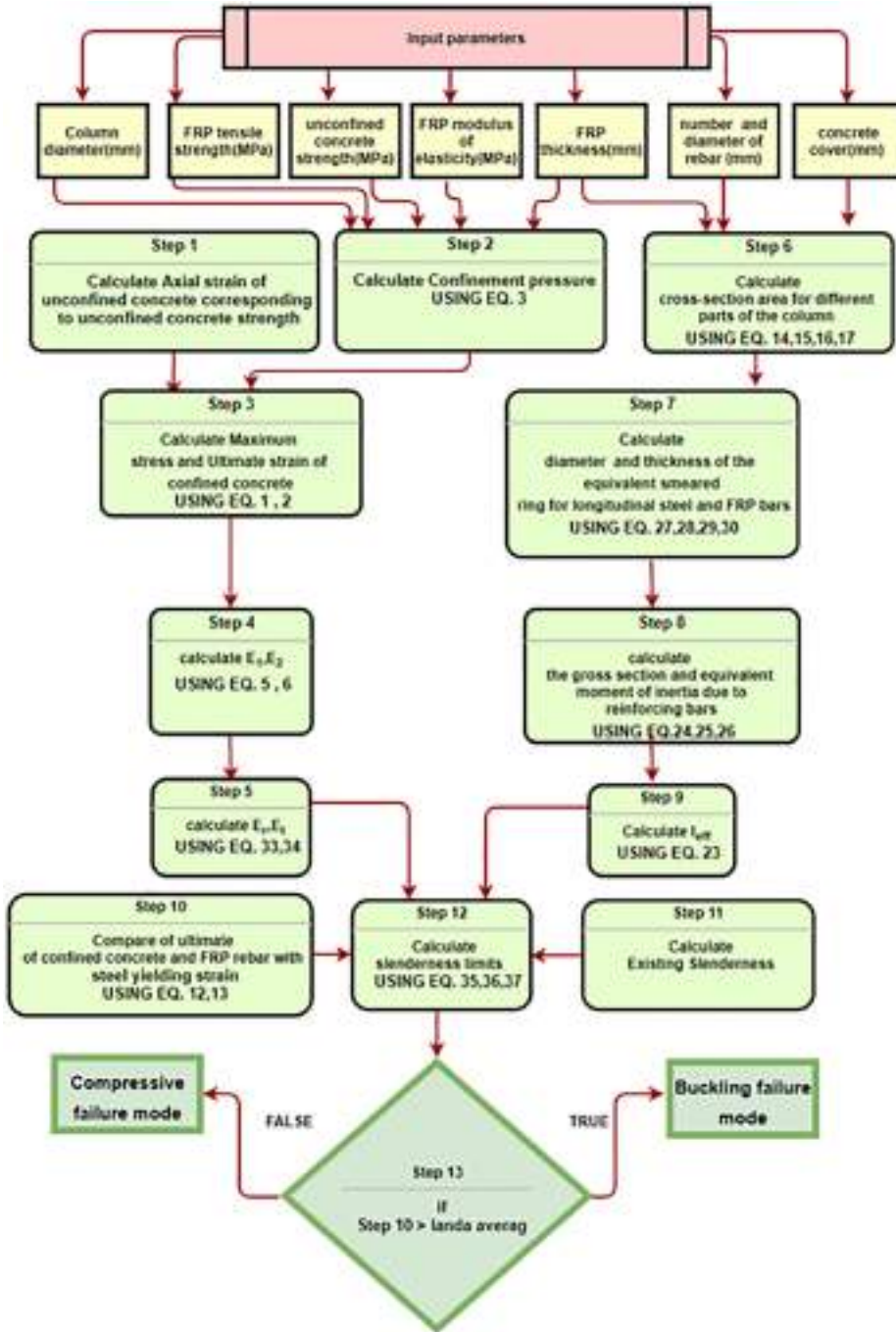## APPENDIX B.: Example for calculation of slenderness limit for a column using the proposed model

FIGURE B1 Flowchart of slenderness limit calculation

TABLE B1 Slenderness limit calculation

	Input parameters								
Diameter	FRP tensile strength	Unconfined concrete strength	FRP modulus of elasticity	FRP thickness	Number of steel/ FRP rebar	Diameter of steel/ FRP rebar	Steel rebar yielding stress	Concrete cover
D(mm)	f_{frp}(MPa)	f_{co}(MPa)	E_{frp}(MPa)	$t_{frpc/l}$(mm)	n	d(mm)	f_y(MPa)	cover **(mm)**
150	846	35.1	77,300	1/0	4/0	8/0	400	25

	Steps
Step 1: calculate ε_{co}	$\varepsilon_{co} = 0.001648 + 1.68e^{-5}f_{co} = 0.00222$
Step 2: calculate f_l	$f_l = \frac{2f_f t_f}{d} = 11.28\, MPa$
Step 3: calculate f_{cc}, ε_{cu}	$f_{cc} = f_{co} + \frac{39f_l}{\ln^2(f_{co})} = 69.84\, MPa$
	$\varepsilon_{cu} = \frac{0.21f_l^{0.68}}{f_{co} - \ln(\varepsilon_{co})} = 0.026$
Step 4: calculate E_1, E_2	$E_1 = 3535\sqrt{f_{co}} - f_{co} = 20908.1\, MPa$
	$E_2 = 1.1\frac{f_{cc}}{\sqrt{\varepsilon_{cu}}} = 1628.03\, MPa$
Step 5: calculate E_r, E_t	$E_r = \left[\frac{1}{2}\left(\frac{1}{\sqrt{E_u}} + \frac{1}{\sqrt{E_t}}\right)\right]^{-2} = 2978.83\, MPa$
	$E_t = E_2 = 1628.03\, MPa$
Step 6: calculate $A_{sb}, A_{fb}, A_{frp_i}, A_c$	$A_{sb} = n_{sb}\frac{\pi\phi_{sb}^2}{4} = 201.06\, mm^2$
	$A_{fb} = n_{fb}\frac{\pi\phi_{fb}^2}{4} = 0$
	$A_{frp_i} = \pi d t_{fl_i} = 471.23\, mm^2$
	$A_c = \frac{\pi\left(d^2 - n_{sb}\phi_{sb}^2 - n_{fb}\phi_{fb}^2\right)}{4} = 17470.4\, mm^2$
Step 7: calculate $d_{sb}, d_{fb}, t_{sb}, t_{fb}$	$d_{sb} = d - 2C_{sb} - \phi_{sb} = 92$
	$d_{fb} = d - 2C_{fb} - \phi_{fb} = 0$
	$t_{sb} = \frac{A_{sb}}{\pi d_{sb}} = 0.69\, mm$
	$t_{fb} = \frac{A_{fb}}{\pi d_{fb}} = 0$
Step8: calculate I_g, I'_b, I'_w	$I_g = \frac{\pi d^4}{64} = 24850489\, mm^4$
	$I'_b = I'_{sb} + I'_{fb} = \frac{\pi}{8}\left[\left(\frac{E_{sb}}{E_c} - 1\right)d_{sb}^3 t_{sb} + \left(\frac{E_{fb}}{E_c} - 1\right)d_{fb}^3 t_{fb}\right] = 1358637\, mm^4$
	$I'_w = \sum_{i=1}^{n}\left(\frac{\pi}{8}\frac{E_{f_i}}{E_c}d^3 t_{fl_i}\right) = 0$
Step 9: calculate I_{eff}	$I_{eff} = \alpha\left(I_g + I'_b\right) + \beta I'_w = 19656844\, mm^4$
	$\alpha = 0.75, \beta = 0.25$
Step 10: compare $\varepsilon_{cu}, \varepsilon_y, \varepsilon_{fb}$	$\varepsilon_y = 0.002$
	$\varepsilon_{cu} = 0.026 \geq \varepsilon_y$ then use ε_y
	$\varepsilon_{fb} = 0$
Step 11: calculate $\lambda_{c\,exist}$	$\lambda_c = \frac{KL}{r} = 16$
Step 12: calculate $\lambda_{ct}, \lambda_{cr}, \lambda_{avg}$	$\lambda_{ct} = \frac{\pi}{r}\sqrt{\frac{E_2 I_{eff}}{f_{cc}A_c + E_{sb}\varepsilon_{cu}A_{sb} + E_{fb}\varepsilon_{cu}A_{fb} + \sum_{i=1}^{n}E_{frp_i}\varepsilon_{cu}A_{frp_i}}} = 9.95$
	$\lambda_{cr} = \frac{\pi}{r}\sqrt{\frac{E_r I_{eff}}{f_{cc}A_c + E_{sb}\varepsilon_{cu}A_{sb} + E_{fb}\varepsilon_{cu}A_{fb} + \sum_{i=1}^{n}E_{frp_i}\varepsilon_{cu}A_{frp_i}}} = 13.46$
	$\lambda_{avg} = \frac{\lambda_{cr} + \lambda_{ct}}{2} = 11.71$
Step 13: comparison of $\lambda_{c\,exist}, \lambda_{avg}$	$\lambda_{c\,exist} > \lambda_{avg}$: *Buckling is mode of failure*

Abbreviation: FRP, FRP, fiber-reinforced polymer.